



Autophagy Induced Accumulation of Lipids in *pgr1* and *pgr5* of *Chlamydomonas reinhardtii* Under High Light

Nisha Chouhan, Elsinraju Devadasu, Ranay Mohan Yadav and Rajagopal Subramanyam*

Department of Plant Sciences, School of Life Sciences, University of Hyderabad, Hyderabad, India

OPEN ACCESS

Edited by:

Milton Lima Neto,
São Paulo State University, Brazil

Reviewed by:

Fantao Kong,
Dalian University of Technology, China
Ayse Kose,

Ege University, Turkey

Justin Findinier,
Carnegie Institution for Science,
United States

*Correspondence:

Rajagopal Subramanyam
srgsl@uohyd.ernet.in

Specialty section:

This article was submitted to
Plant Abiotic Stress,
a section of the journal
Frontiers in Plant Science

Received: 03 August 2021

Accepted: 20 December 2021

Published: 25 January 2022

Citation:

Chouhan N, Devadasu E,
Yadav RM and Subramanyam R
(2022) Autophagy Induced
Accumulation of Lipids in *pgr1*
and *pgr5* of *Chlamydomonas*
reinhardtii Under High Light.
Front. Plant Sci. 12:752634.
doi: 10.3389/fpls.2021.752634

Chlamydomonas (C.) reinhardtii is a potential microalga for lipid production. Autophagy-triggered lipid metabolism in microalgae has not been studied so far from a mutant of proton gradient regulation 1 like (PGR1) and proton gradient regulation 5 (PGR5). In this study, *C. reinhardtii* cells (wild-type CC124 and cyclic electron transport dependent mutants *pgr1* and *pgr5*) were grown photoheterotrophically in high light 500 $\mu\text{mol photons m}^{-2} \text{s}^{-1}$, where *pgr5* growth was retarded due to an increase in reactive oxygen species (ROS). The lipid contents were increased; however, carbohydrate content was decreased in *pgr5*. Further, the Nile Red (NR) fluorescence shows many lipid bodies in *pgr5* cells under high light. Similarly, the electron micrographs show that large vacuoles were formed in high light stress despite the grana stacks structure. We also observed increased production of reactive oxygen species, which could be one reason the cells underwent autophagy. Further, a significant increase of autophagy ATG8 and detections of ATG8-PE protein was noticed in *pgr5*, a hallmark characteristic for autophagy formation. Consequently, the triacylglycerol (TAG) content was increased due to diacylglycerol acyltransferases (DGAT) and phospholipid diacylglycerol acyltransferase (PDAT) enzymes' expression, especially in *pgr5*. Here the TAG synthesis would have been obtained from degraded membrane lipids in *pgr5*. Additionally, mono, polyunsaturated, and saturated fatty acids were identified more in the high light condition. Our study shows that the increased light induces the reactive oxygen species, which leads to autophagy and TAG accumulation. Therefore, the enhanced accumulation of TAGs can be used as feedstock for biodiesel production and aqua feed.

Keywords: *Chlamydomonas reinhardtii*, cyclic electron transport, lipid bodies, Nile Red fluorescence, triacylglycerol

INTRODUCTION

Light is vital for microalgae for efficient photosynthesis. CO_2 fixation by Calvin Benson cycle occurs through photosynthesis that primarily synthesizes carbohydrates, leading to the synthesis of lipid stored as triacylglycerols (TAG) (Mondal et al., 2017). Microalgal species do not accumulate increased amounts of neutral lipids under normal growth conditions. Neutral lipid is accumulated under unfavorable conditions like nutrient, light, salt, and temperature stresses. Under normal light

conditions, the rate of light absorbed is equal to the pace of photosynthesis, but when light intensity increases, the system cannot tolerate over-excitation. In this condition, the primary by-product of photosynthesis formed as reactive oxygen species (ROS), which regulate the autophagy (ATG) mechanism. Autophagy is a stress-responsive mechanism that can induce organelle deterioration (Liu and Bassham, 2012). This mechanism in *Chlamydomonas reinhardtii* regulates the degradative process in photosynthetic organisms. Autophagy plays a divulged role in the control of lipid metabolism. Inhibition of Target of Rapamycin (TOR) kinase by treatment of *C. reinhardtii* cells with rapamycin resulted in increased ATG8 lipidation (Pérez-Pérez et al., 2010) and vacuolization (Pérez-Pérez et al., 2010). Previous results have proven that ROS is an inducer of autophagy in algae (Pérez-Pérez et al., 2010). High light stress induces photo-oxidative damage due to ROS production, leading to autophagy activation in *C. reinhardtii* (Pérez-Pérez et al., 2010). A recent report has shown that a starchless mutant of *C. reinhardtii* induces oxidative stress, triggering autophagy, leading to TAG accumulation under nitrogen starvation (Pérez-Pérez et al., 2012). In a group of ATG (autophagy-related) proteins, the accumulation of ATG8 and ATG3 increased in a conditional repression line of a chloroplast protease (ClpP1), suggesting the chloroplast proteolysis systems and autophagy partially complement each other in *C. reinhardtii* (Ramundo et al., 2014). Additionally, these proteins were shown a similar function to that of other organisms (Pérez-Pérez et al., 2010, 2016). Loss of cytoplasmic structure with a significant increase in the volume occupied by lytic vacuoles and discharge of vacuole hydrolases can be assigned as autophagic cell death markers (Van Doorn, 2011). However, the mechanism of autophagy caused by high light stress in *C. reinhardtii* is poorly understood.

Additionally, it can achieve neutral lipid accumulation by exposing the cells to unfavorable conditions, such as removing the nutrients like nitrogen, sulfur, iron, or phosphate, or changing salinity and temperature (Alishah Aratboni et al., 2019). Most of the knowledge on TAG metabolism in *C. reinhardtii* has been gained from the N starvation (Siaut et al., 2011; Abida et al., 2015). Recent studies showed that cells exposed to small chemically active compounds could also accumulate TAG in *C. reinhardtii* (Wase et al., 2019). However, an increase in light intensity influences the microalgal lipid production in *Scenedesmus* at 6,000 lux (Mandotra et al., 2016), as well as *Nannochloropsis* sp at 700 $\mu\text{E m}^{-2} \text{s}^{-1}$ (Pal et al., 2011) and *Botryococcus* sp. at 6,000 lux (Yeesang and Cheirsilp, 2011). Further, *Haematococcus pluvialis* (Zhekisheva et al., 2002), *Tichocarpus crinitus* (Khotimchenko and Yakovleva, 2005), and *Synechocystis* sp. (Cuellar-Bermudez et al., 2015) also showed an increased neutral lipid content under high light conditions.

Lipid bodies are synthesized in algal chloroplast by fatty acid synthase complex. These newly synthesized free fatty acids are translocated to the endoplasmic reticulum (ER), where they convert glyceraldehyde 3-phosphate (G3P) to diacylglycerol (DAG) through various enzymes. DAG is converted to triacylglycerol by the diacylglycerol acyltransferases (DGAT) enzyme. So, the enzyme is considered to reinforce the assembly of

lipids in microalgae. DGAT enzyme catalyzes the TAG synthesis pathway's ultimate step, and phospholipid diacylglycerol acyl-transferase (PDAT) also helps accumulate TAG. However, it does not hook into the acyl CoA pathway. Here, PDAT transfers carboxylic acid moiety from a phospholipid to DAG to make TAG (Sorger and Daum, 2002; Shockey et al., 2006). A recent report from our group shows that a significant accumulation of TAG was observed under severe iron deficiency, and this could have been obtained from degraded chloroplast lipids through the DGAT enzyme (Devadasu et al., 2021).

Few studies have focused on increased fatty acid content, decreased photosynthetic activity, and retarded biomass, ultimately inhibiting microalgae growth in nutrient limitation. *pgr1* is required for efficient cyclic electron transport (CET) and adenosine triphosphate (ATP) supply for efficient photosynthesis (Tolte et al., 2011; Leister and Shikanai, 2013; Shikanai, 2014; Steinbeck et al., 2015). A *pgr5* mutant has been characterized in *C. reinhardtii* (Johnson et al., 2014), which revealed that *pgr5* deficiency results in a diminished proton gradient across the thylakoid membrane accompanied by less effective CET capacity. The CET pathway has been suggested to provide ATP for lipid production during N starvation in *C. reinhardtii* mutants impaired in *pgr1*, which accumulates significantly fewer neutral lipids. However, under the high light condition, there is an increase in oil content after the 3rd day. So far, the accumulation of lipids has been well characterized in nutrient stress; however, not many studies are available under high light conditions. In *C. reinhardtii* (WT) the solar light is transformed into chemical energy using linear electron transport. However, *pgr1* and *pgr5*, may show an increase in stromal redox poise that would cause an increase in lipid production under strong light.

In this study model, algae *C. reinhardtii* was propagated with different light conditions (50 and 500 $\mu\text{mol photons m}^{-2} \text{s}^{-1}$) to realize insights into the autophagy and lipid accumulation response to high light. We propose that *C. reinhardtii* cells exposure to high light resulted in ROS accumulation, which induced autophagy and lipid accumulation in *pgr5*.

MATERIALS AND METHODS

Strains and Culture Conditions

The green microalgae *C. reinhardtii* wild-type (WT) strain CC124 (137c) was obtained from the *C. reinhardtii* resource center (University of Minnesota) and mutants *pgr1* and *pgr5* (137c background; Johnson et al., 2014), a kind of gift from Prof. Gilles Peltier (CEA-CNRS- Aix Marseille University, France) and Prof. Michael Hippler (University of Munster, Germany). Cells were grown photoheterotrophically in Tris-acetate phosphate (TAP) medium at 25°C with a photon flux density of 50 $\mu\text{mol photons m}^{-2} \text{s}^{-1}$ in 250 mL conical flask shaken at 120 rpm in an orbital shaker at 25°C. The seed cultures of *C. reinhardtii* (WT, *pgr1*, and *pgr5*) were harvested at an optical density (OD) of 0.8 and inoculated at OD of 0.02 for all the cultures. The cultures were cultivated photoheterotrophically at 25°C for 4 days at a continuous light intensity of 50 and 500 $\mu\text{mol photons m}^{-2} \text{s}^{-1}$. Later the cultures were collected after the 3rd day with an OD of

0.8 at 750 nm. Light intensity was measured and adjusted with a light meter (Hansatech).

Biomass Determination

To calculate the total biomass of cells (WT and mutants *pgrl1* and *pgr5*), 5 mL of culture was collected after the 3rd day of growth in high light and control by centrifugation at $1,000 \times g$ for 10 min at room temperature (RT), and the supernatant was discarded. The excess media was removed by short centrifugation, and cell pellets were lyophilized at -109°C for 12 h. The cell pellet was washed with distilled water and transferred into a pre-weighed 15 mL falcon tube. The total dry weight was later quantified by subtracting the empty tube.

Reactive Oxygen Species Measurement

The total ROS was detected with 2,7-dichlorodihydrofluorescein diacetate (H_2DCFDA) (Sigma-Aldrich), a fluorescence dye used to see the ROS in live *C. reinhardtii* cells. Cells at a 3 million density were collected from all the conditions, and H_2DCFDA staining was performed at $10 \mu\text{M}$ concentration (Upadhyaya et al., 2020). Further, cells were incubated with dye for 1 h at RT in a continuously rotating shaker under dark. Images were captured using Carl Zeiss NL0 710 Confocal microscope. H_2DCFDA was detected in a 500–530 nm bandpass optical filter with an excitation wavelength of 492 nm and an emission wavelength of 525 nm. Chlorophyll auto-fluorescence was detected using an optical filter of 600 nm. Samples were viewed with a $60\times$ oil immersion lens objective by using the ZEN, 2010 software.

Total ROS produced by *C. reinhardtii* cells was also quantified by spectrophotometer. Logarithmic-phase cells were centrifuged at $1,500 \times g$, 20°C for 5 min, resuspended in an equal volume of fresh TAP medium, and then incubated in $5 \mu\text{M}$ DCFH-DA for 1 h in the dark at 25°C . After dark exposure, the cells were washed twice with TAP to remove excess dye (Devadasu et al., 2019). The fluorescence was measured using a Microplate reader (Tecan M250) at an excitation of 485 nm and an emission of 530 nm. We calculated the total ROS by subtracting the value of fluorescence with dye and without dye.

Transmission Electron Microscopy

The cells (3×10^6 cells/ml) were resuspended in 0.1 M phosphate buffer (pH 7.2). Cells were fixed in a 2% Glutaraldehyde (Sigma-Aldrich, St. Louis, United States) solution for 2 h in the dark. The cells were then washed four times in PBS buffer for 1 h each time before being post-fixed in 2% aqueous Osmium Tetraoxide for 3 h, washed six times in deionized distilled water, dehydrated in a series of ethanol solutions (30, 50, 70, and 90%, and three changes of 100% for 10 min each), infiltrated, and embedded in Araldite resin. Ultra-thin sections (60 nm) were cut with a glass ultramicrotome (Leica Ultra cut UCT-GA-D/E-1/100) and placed on copper grids after incubation at 80°C for 72 h for complete polymerization. The sections were stained with uranyl acetate and counterstained with Reynolds lead citrate, with some alterations (Bozzola and Russell, 1998). A Hitachi 7500 (Japan) transmission electron microscope was used to take the images.

Localization of ATG8 From Immunofluorescence Microscopy

For immunofluorescence, cells (3×10^6 cells/ml) were fixed in a solution of 4% paraformaldehyde and 15% sucrose dissolved in phosphate saline buffer (PBS) for 1 h at RT. Later, the cells were washed twice with PBS buffer. First, cells were permeabilized by incubation in 0.01% Triton X100 in PBS for 5 min at RT and washed twice in PBS. Next, the samples were transferred to sterile Eppendorf tubes and blocked with a 1% BSA (w/v) in PBS for 1 h. Samples were incubated with anti-ATG8 diluted (1:1000) in PBS buffer, pH = 7.2 containing 1% BSA overnight at 4°C on a rotatory shaker. Cells were then washed twice with PBS for 10 min at 25°C , followed by incubation in a 1:10000 dilution of the fluorescein Dylight 405 labeled goat anti-rabbit secondary antibody (Sigma) in PBS-BSA for 2 h at 25°C . Finally, cells were washed three times with PBS for 5 min. Images were captured with Carl Zeiss NL0 710 Confocal microscope. ATG8 localization was detected with excitation of Dylight 405 nm and emission at 420 nm by analyzing the images with ZEN software.

Lipid Body Analysis by Nile Red Staining

We studied the impact of high light on non-polar lipid accumulation with confocal microscopy. Cells (3×10^6 cells/ml) were collected after the 3rd-day growth in high light along with control. To stop the mobility of the cells, $5 \mu\text{L}$ Iodine solution [0.25 g in ethanol (95%)] was mixed and kept for 5 min under dark at RT. The cell suspension was then stained with Nile Red (NR, $1 \mu\text{g mL}^{-1}$ final concentration, Sigma, Sigma-Aldrich) followed by 20 min incubation in the dark. After staining, the samples were placed on a glass slide with a coverslip. Images were captured using Carl Zeiss NL0 710 confocal microscope. A 488 nm scanning laser was used with a 560–615 nm filter to detect neutral lipids. Samples were viewed with a $60\times$ oil immersion lens objective, and the ZEN, 2010 software package was used for image analysis.

Nile Red Visible Light Assay for Triacylglycerol

The *C. reinhardtii* cultures were diluted to a density of 3.0×10^6 cells mL^{-1} and placed within 96 well microplate wells. To every well, a $5 \mu\text{L}$ aliquot of $50 \mu\text{g mL}^{-1}$ NR; (Sigma; ready in acetone) was added in $200 \mu\text{L}$ of equal density cells (3.0×10^6 cells mL^{-1}), and after a thorough mix, the plate was incubated in the dark for 20 min. The neutral lipids were then measured by visible light at a 485-nm excitation filter and a 595-nm emission filter employing a plate reader (Tecan infinite M200, Magellan). Quantification was achieved by using a standard curve ready with the lipid Triolein (Sigma T4792).

Flow Cytometry Measurements

Flow cytometer Calibur (BD Falcon, United States) was used to quantify neutral lipid stain with NileRed. Cells were stained with $1 \mu\text{g mL}^{-1}$ NR ($100 \mu\text{g mL}^{-1}$ stock in acetone) in the dark for 30 min before flow cytometry analysis. Measurement of 10,000 cells per sample was analyzed without gating and auto-fluorescence was nullified before measuring the NR fluorescence.

The fluorescence reading was obtained at a 488-nm excitation filter and a 545-nm emission. The distribution of the cells stained with NR was expressed as a percent of the total.

Total Pigment and Carbohydrate Quantification

C. reinhardtii cells were harvested by centrifugation ($1,000 \times g$ for 10 min) after the 3rd day at a cell density of 3.0×10^6 . Cell pellets were resuspended in methanol for chlorophyll extractions. The supernatant was used to measure the total chlorophyll (Porra et al., 1989). To calculate total carotenoid cell pellets were resuspended in 80% acetone, and the supernatant was used to measure the total carotenoid. Absorbance was measured at wavelength 480, 663, and 645 nm. Total carotenoid was calculated as $= A_{480} + 0.114 (A_{663}) - 0.638(A_{645})$ (Wellburn, 1952). Total carbohydrate was quantified by an Anthrone method (plate reader assay). For quantification of carbohydrate, the cell pellet was resuspended in 50 μ L Milli-Q water and 150 μ L of Anthrone chemical agent (0.1 g in 100 mL of conc. H_2SO_4 98%) was added to the 50 μ L algal cells. Initially, plates were incubated at 4°C for 10 min and then incubated at 100°C for 20 min. Later on, plates were placed at RT until color development. Plates were measured at 620 nm on an assay plate reader (Tecan M250), and total carbohydrate was calculated (Wase et al., 2019).

LIPID ANALYSIS AND QUANTIFICATION

For lipid extraction, 5-mg of lyophilized dry biomass was weighed equally from all the conditions. Total lipids were extracted as described by Bligh and Dyer's method (Bligh and Dyer, 1959). Cell powder was resuspended in a mixture of methyl alcohol, chloroform (2:1), and 0.9% KCl. It was vortexed for 5 min and centrifuged at $3,000 \times g$ for 5 min for phase separation. The organic layer (lower layer phase) was transferred to a clean Eppendorf tube. The solvent was evaporated by purging nitrogen gas. The dried extract was then dissolved in 50 μ L chloroform. For standard, TAG (Sigma-Aldrich, St. Louis, United States) was dissolved in $CHCl_3$ (1 mg mL^{-1}). Around 0.5 μ g of lipid extract was loaded as a spot on 20 cm \times 20 cm silica gel TLC plates. For neutral lipids separation, the TLC plate was developed in a mixture of hexane/diethyl ether/acetic acid (17:3:0.2), and polar lipids (membrane lipids) were developed in a mixture of acetone/toluene/water (91:30:8) according to Wang and Benning (2011). Bands were visualized by staining with iodine vapor and identified the membrane lipids as cited above. For quantitative analysis, individual lipids were extracted from the TLC plates with a razor blade transferred into a glass tube followed by *trans* methylation to fatty acid methyl esters (FAMES). FAME of the samples were identify quantitatively by GC (gas chromatographs) 6,890 fitted with 25 m \times 0.2 mm phenylmethyl silicone fused silica capillary. The temperature program ramps from 170 to 270°C at 5°C per min. Following the analysis, a ballistic increase to 300°C allows cleaning of the column during a hold of 2 min. The amounts of fatty acids were calculated based on the content of fatty acids derived

from GC using heptadecanoic acid (Sigma-Aldrich, St. Louis, United States) as an internal standard.

Fatty Acid Methyl Esters Analysis for the Total Lipids

The 5 mg lyophilized sample was dissolved in 1,000 μ L of acetonitrile (ACN), 0.1% formic acid (FA) (v/v), and vortexed for 1 h at 900 rpm at RT. The solution was then centrifuged at 13,000 rpm for 10 min at 4°C. 100 μ L of supernatant was collected, and the pellet was dried using a speed vacuum. The pellet was dissolved in 90 μ L of acetonitrile 0.1% formic acid (v/v) and spiked with 10 μ L of the standard internal mixture (Table 1). The solution was vortexed for 30 min at 750 rpm at RT and speed vacuumed to dry at 40°C. The extracted lipids were derivatized with *n*-Butanol for 20 min at 60°C, then again speed vacuumed to dry at 60°C for 15 min. The dried pellets were dissolved in 100 μ L of ACN 0.1% FA and vortexed for 5 min at 750 rpm on a thermomixer. The samples were then centrifuged at 13,000 rpm for 10 min at RT. The supernatant was taken into HPLC sample vials for further analysis. The 100 μ L extracted lipid samples were brought to RT and filled into individual HPLC vials with 200 μ L inserts and placed into the autosampler of Nexera X2 UFLC, connected to LC-MS/MS (SHIMADZU 8045) MS system with an ESI source. The data was analyzed by Lab solutions software, and the concentrations were calculated by measuring the area under the curve (AUC) for the internal standards.

Immunoblots

Cells were collected by centrifugation. The cell pellet was solubilized in protein extraction buffer (0.1 M DDT, 4% SDS, and 0.1 M Tris, pH- 7.6), and all the samples were kept for heating at 95°C for 5 min. Cell suspensions were centrifuged at $2,810 \times g$ for 10 min, and the supernatant was collected. Protein concentration was quantified using the Bradford method, and 5 μ g of proteins were loaded per well. The individual proteins were separated with 15% Bis-Tris gels for diacylglycerol acyltransferases (DGAT2A) and PDAT1 proteins and 12% for ATG8 and Histone3 (H3) proteins. Separated proteins were then transferred to a nitrocellulose membrane (Towbin et al., 1979). Specific primary antibodies were purchased from Agrisera (Sweden) and used at dilutions of DGAT2A (1:2500), PDAT (1:2500), and ATG8 (1:2500). H3 (1:10,000) was used to see equal loading. The secondary antibody, anti-IgG raised from Goat (1:10,000), was used for detection. Immunoblots were obtained by the Chemi-Doc touch imaging system (Bio-Rad) by using Chemiluminescence.

Statistical Analysis

All experiments were conducted in triplicate, and data are obtained as the mean \pm standard deviation (SD). Statistical analysis was done using Sigma plot 14.5 software. One-way ANOVA and subsequent Tukey Test were used to analyze the statistical significance ($*p < 0.05$, $**p < 0.01$, $***p < 0.001$) of the data.

TABLE 1 | Fatty acid content of *C.reinhardtii* under normal and high light conditions.

Fatty acid	WT	WT	<i>pgr1</i>	<i>pgr1</i>	<i>pgr5</i>	<i>pgr5</i>
	(50 $\mu\text{mol photons m}^{-2} \text{ s}^{-1}$) % \pm S.D	(500 $\mu\text{mol photons m}^{-2} \text{ s}^{-1}$) % \pm S.D	(50 $\mu\text{mol photons m}^{-2} \text{ s}^{-1}$) % \pm S.D	(500 $\mu\text{mol photons m}^{-2} \text{ s}^{-1}$) % \pm S.D	(50 $\mu\text{mol photons m}^{-2} \text{ s}^{-1}$) % \pm S.D	(500 $\mu\text{mol photons m}^{-2} \text{ s}^{-1}$) % \pm S.D
C14:0	0.237 \pm 0.003	0.546 \pm 0.004	0.185 \pm 0.001	0.176 \pm 0.001	0.594 \pm 0.003	0.609 \pm 0.003
C14:1	0.182 \pm 0.002	0.589 \pm 0.005	0.423 \pm 0.002	0.154 \pm 0.001	0.329 \pm 0.002	0.508 \pm 0.003
C14:2	0.296 \pm 0.003	0.767 \pm 0.003	0.423 \pm 0.002	0.132 \pm 0.001	0.632 \pm 0.003	0.406 \pm 0.002
C14:3	0.123 \pm 0.002	0.412 \pm 0.003	0.318 \pm 0.002	0.64 \pm 0.003	0.228 \pm 0.001	0.216 \pm 0.001
C16:0	1.182 \pm 0.002	1.412 \pm 0.003	2.123 \pm 0.007	3.415 \pm 0.007	3.45 \pm 0.005	7.132 \pm 0.006
C16:1	1.070 \pm 0.006	2.391 \pm 0.021	1.874 \pm 0.004	4.178 \pm 0.006	2.212 \pm 0.003	4.398 \pm 0.001
C16:2	0.192 \pm 0.002	1.764 \pm 0.004	0.36 \pm 0.002	2.544 \pm 0.003	0.573 \pm 0.003	5.027 \pm 0.005
C16:3	1.213 \pm 0.019	4.76 \pm 0.008	1.816 \pm 0.009	2.78 \pm 0.014	2.1 \pm 0.010	3.13 \pm 0.016
C18:0	0.499 \pm 0.002	1.12 \pm 0.004	1.659 \pm 0.008	2.061 \pm 0.012	1.025 \pm 0.005	3.752 \pm 0.007
C18:1	0.168 \pm 0.001	0.942 \pm 0.003	0.439 \pm 0.002	1.998 \pm 0.004	0.826 \pm 0.004	5.46 \pm 0.012
C18:2	0.427 \pm 0.002	0.200 \pm 0.001	0.651 \pm 0.003	0.212 \pm 0.001	0.199 \pm 0.003	1.15 \pm 0.003
C18:3	3.124 \pm 0.018	7.200 \pm 0.029	2.725 \pm 0.029	5.895 \pm 0.014	5.738 \pm 0.109	7.266 \pm 0.046
C18:4	1.21 \pm 0.005	2.56 \pm 0.019	2.114 \pm 0.011	1.23 \pm 0.006	3.161 \pm 0.04	3.395 \pm 0.017
Σ SFA	1.918 \pm 0.016	3.078 \pm 0.007	3.967 \pm 0.016	5.652 \pm 0.02	5.069 \pm 0.02	11.493 \pm 0.016
Σ MUFA	1.42 \pm 0.007	3.92 \pm 0.008	2.736 \pm 0.027	5.33 \pm 0.019	3.367 \pm 0.011	10.36 \pm 0.025
Σ PUFA	4.192 \pm 0.051	17.46 \pm 0.059	8.407 \pm 0.203	12.43 \pm 0.072	12.631 \pm 0.042	20.59 \pm 0.09
Σ TFA	7.53 \pm 0.079	24.45 \pm 0.091	15.11 \pm 0.252	25.415 \pm 0.101	21.067 \pm 0.073	42.449 \pm 0.131

The data represents as % of total fatty acid for $n = 3$. SFA, saturated fatty acids; MUFA, monounsaturated fatty acids; PUFA, polyunsaturated fatty acids; TFA, total fatty acids.

RESULTS

Growth and Pigment Analysis Under High Light

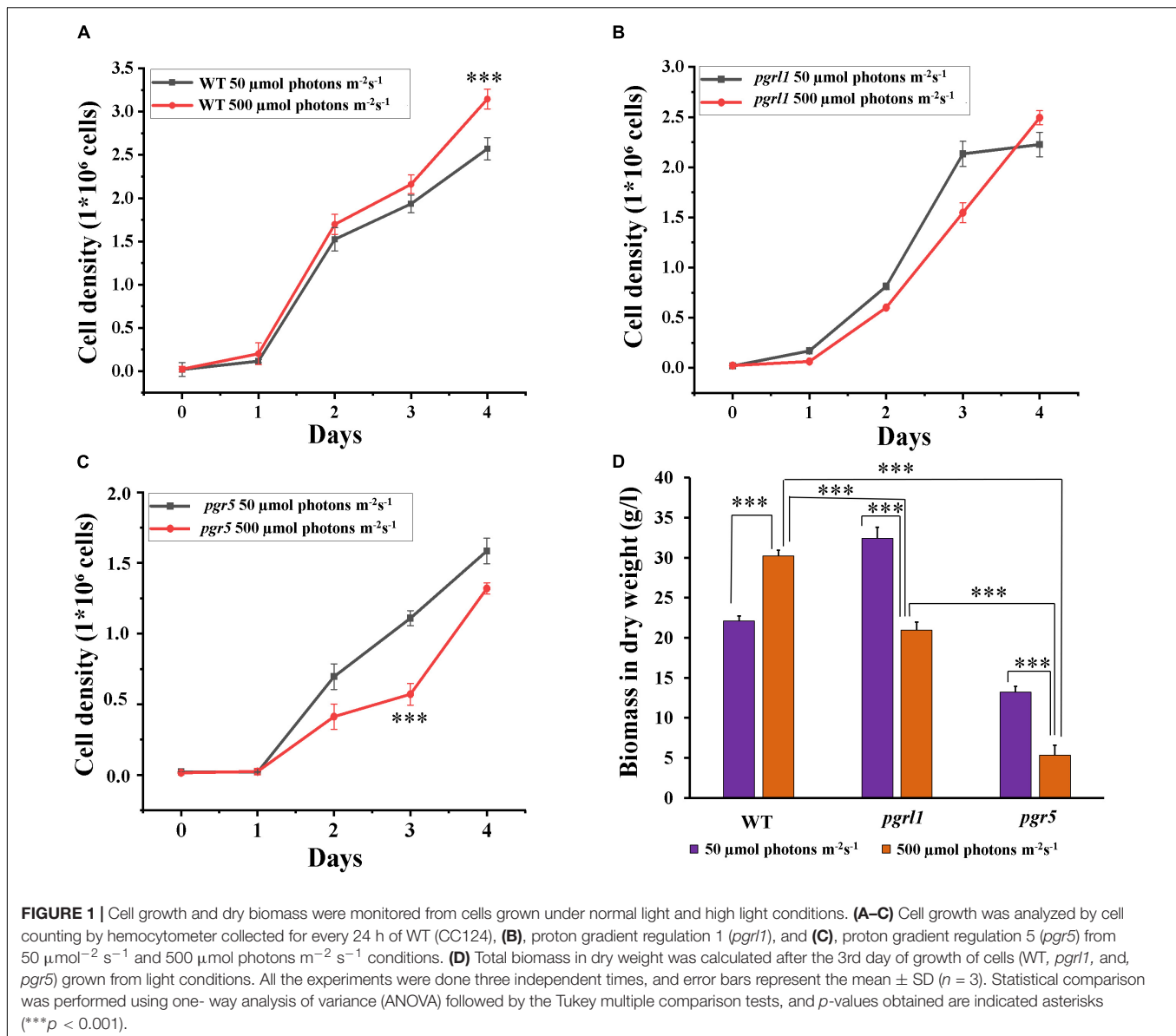
The WT, proton gradient regulation (*pgr1*) and *pgr5* (cyclic electron transport dependant mutants) were grown in Tris-acetate phosphate (TAP) medium at light intensities of 50 (as a control) and 500 $\mu\text{mol photon m}^{-2} \text{ s}^{-1}$ for 4 days. Under 50 $\mu\text{mol photon m}^{-2} \text{ s}^{-1}$ light intensity, all the cultures grew normally (Figure 1). The growth of WT cultures increased (Figure 1A), but *pgr1* and *pgr5* mutants exhibited slower growth in high light conditions after 2 days (Figures 1A–C). Our results showed that the cell growth pattern of the WT was increased 30%, whereas *pgr1* and *pgr5* growth were decreased 21 and 30% compared to the WT under high light (500 $\mu\text{mol photon m}^{-2} \text{ s}^{-1}$) after 3rd day and normalized OD data was shown in Supplementary Table 1. Mainly, the *pgr5* mutant shows impaired growth, whereas *pgr1* was not affected under the same high light condition (500 $\mu\text{mol photon m}^{-2} \text{ s}^{-1}$) after 3rd day of growth (Figures 1B,C). We have studied the effect of light intensity on biomass. The WT shows an increase in biomass yield 75.5% in high light, however, it reduced 64.6 and 43.6% in *pgr1* and *pgr5*, respectively, after the 3rd day (Figure 1D). However, after the 4th day, biomass is almost the same in both mutants when grown in high light.

To determine the effect of high light on the pigment level associated with *C. reinhardtii* photosynthetic complex, we have measured the chlorophyll and carotenoid content from standard and high light-grown cells. Chlorophyll content was significantly reduced in *pgr1* and *pgr5* mutants, respectively, under high light intensity (Figure 2A). At the same time, we observed

twofold increase in carotenoid content in *pgr1* and *pgr5* under high light (Figure 2B). It is known that increased carotenoid content acts as a protective mechanism against light stress in the *C. reinhardtii* (Li et al., 2009). Carotenoids under high light conditions generally tend to increase to protect PSII from photoinhibition. Data shows that an increase in light intensity results in decreased specific growth rate, increased carotenoid, and reduced biomass production of *pgr1* and *pgr5*. We assume that reduced growth might be due to ROS production. Our results have elicited us to check further studies and detect the ROS in high light stress.

Reactive Oxygen Species Induction in High Light

To determine the oxidative stress, cells were stained with 2',7'-dichlorodihydrofluorescein diacetate (H₂DCFDA). ROS was observed using confocal microscopy as well as quantified by spectrophotometry (Figures 3A,C), where an increase in ROS was observed under the high light condition in WT, *pgr1*, and *pgr5* (Figure 3). However, this increase was predominant in *pgr5* (Figures 3A–C). The generation of more ROS in *pgr5* could probably explain the reduced growth rate. Further, these results suggest that ROS formation under high light may contribute to autophagy and lipid accumulation. Reports show that ROS may induce multiple metabolic functions like lipid metabolism and autophagy (Shi et al., 2017). High light is one of the factors responsible for ROS formation because of over reduction of the photosynthetic electron transport chain, which might generate ROS that induces autophagy in *C. reinhardtii* (Pérez-Pérez et al., 2012). Based on the above reports, we have conducted experiments related to autophagy caused by high light.



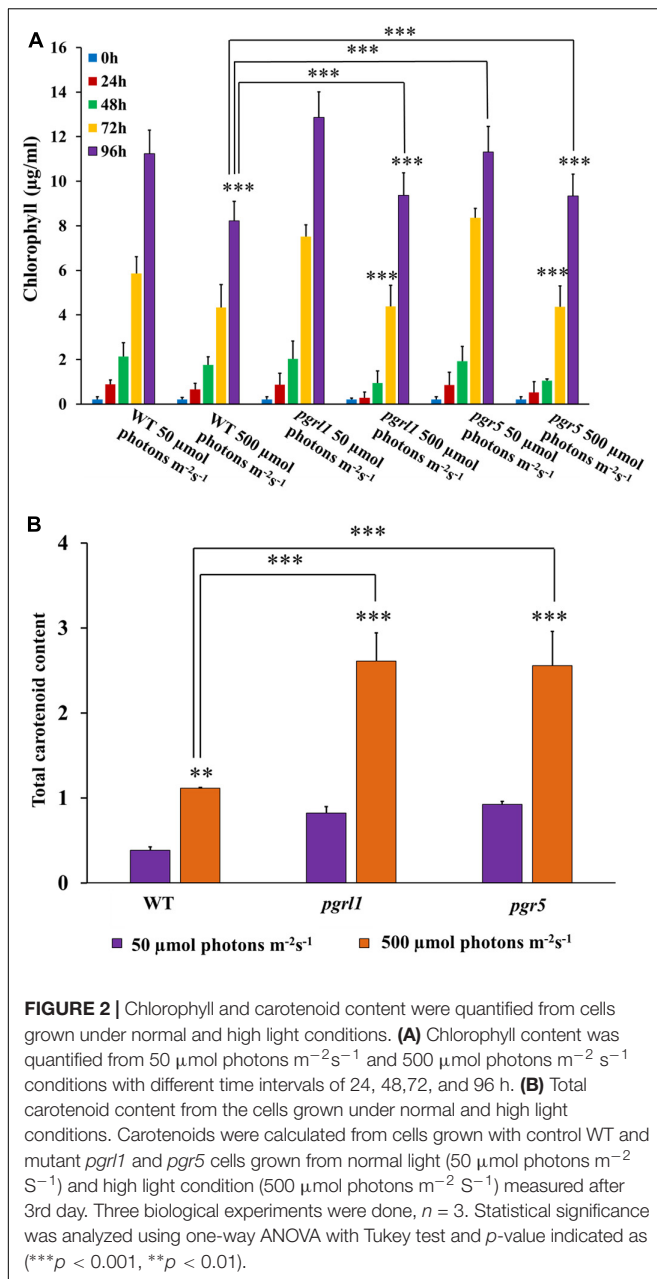
Cellular Localization of ATG8

We have used an anti-ATG8 antibody to examine this protein's cellular localization in immunofluorescence microscopy (Figure 4A). Autophagy (ATG8) proteins localize as small red dots in the cytoplasm under the normal light condition in WT, *pgr11*, and *pgr5* mutant. However, under high light conditions, number of spot significantly increased in *pgr5* (40%) (Supplementary Figure 1), which shows activation of autophagy and formation of autophagosomes in close agreement with high accumulation of ATG8 [phosphatidylethanolamine (PE) modified ATG8] detected by western blotting. The autophagy-related protein ATG8-PE was significantly expressed in *pgr5* in high light conditions (Figures 4B,C). Upon autophagy activation, ATG8 binds to the autophagosome membrane through phospholipid phosphatidylethanolamine (PE) to form ATG8-PE in a process called lipidation. Hence autophagy may

play a significant role in the accumulation of lipids in high light conditions in *pgr5*. Therefore, in line with autophagy, the accumulation of lipids is lower in WT and *pgr11*. However, the ATG8 expression is predominant in *pgr5* under high light conditions. These results suggested that induction of ROS due to high light may induce autophagy in *pgr5* than WT and *pgr11* (Pérez-Pérez et al., 2012; Perez-Martin et al., 2014). Therefore, it may trigger the lipid metabolism in *C. reinhardtii* cells.

Lipid Droplet Analysis From Confocal Microscopy

We have stained the cells with Nile red (NR) for lipid studies, binds explicitly to lipid bodies in the cell, and gives a characteristic yellow-orange fluorescence. Our results clearly show the overall increase of lipid droplets under high light in WT, *pgr11*, and *pgr5* mutants (Figures 5A,B and



Supplementary Figure 2). When we measure the fluorescence intensity from the confocal images, the number of lipid spots is higher in high light-grown cells, but it is more significant in *pgr5* (Figure 5C). However, autofluorescence due to chlorophyll was less in *pgr11* and *pgr5* than in control, indicating decreased chlorophyll content under high light, even though cells had a significant accumulation of lipid bodies (Figure 5A). Lipid accumulation was observed in all strains under high light conditions (Goold et al., 2016). However, lipid accumulation is more significant in *pgr5* (60%) than other strains under high light. We have tested NR fluorescence from fluorescent activated cell sorter (FACS) to assess the lipid accumulation in high light conditions. We obtained twofold higher mean fluorescence

intensity from all the strains with high light than normal growth conditions (Figure 5D).

Neutral Lipid Identification by Nile Red Fluorescence

The neutral lipids were semi-quantified by using NR fluorescence from an equal number of cells. NR fluorescence results show that the neutral lipid level was increased with equal cell density. NR fluorescence of *C. reinhardtii* cells WT, *pgr11*, and *pgr5* were calculated every 24 h while growing them in light at 50 and 500 $\mu\text{mol photon m}^{-2}\text{s}^{-1}$ (Supplementary Figure 3). After 24 h, cells did not cause any change in total lipid content. However, after 48 h of high light growth, there was an increase in NR fluorescence.

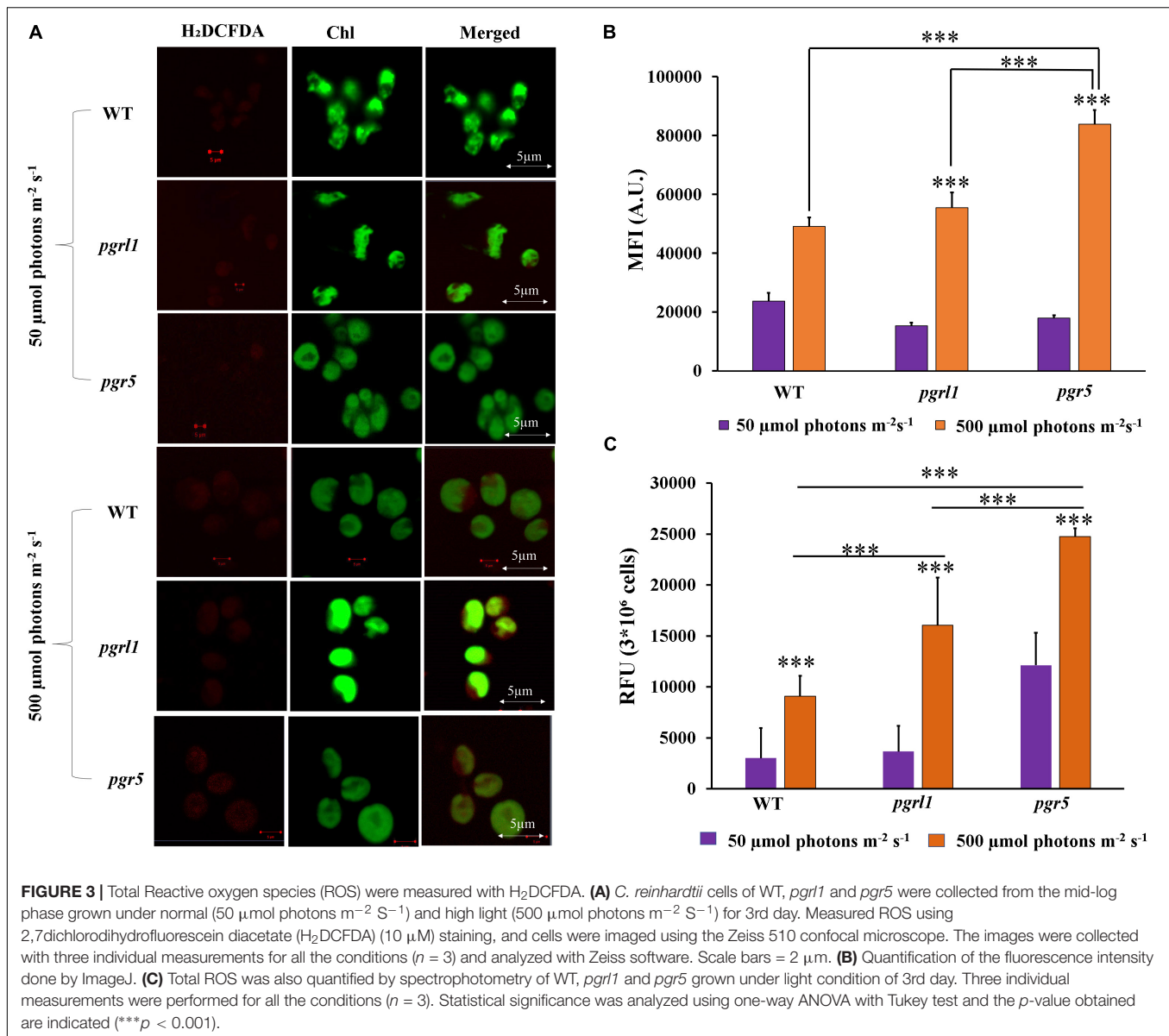
In contrast, there is an increase in signal at 750 nm. Overall, high light-grown cells exhibit a relative two-fold increase in neutral lipid content over 3–4 days. However, this accumulation of neutral lipids is predominantly more in the *pgr5* mutant when compared to other strains. Therefore, our results indicate that an increase in light intensity facilitates the production of neutral lipids in *C. reinhardtii*. Further, we have performed electron microscopic studies to determine whether high light induces lipid accumulation in the cells.

Transmission Electron Microscopy Studies

To see the clear lipid vacuoles in the cell, we have carried out transmission electron microscopy (TEM). It reveals that *pgr11* and *pgr5* exhibit a large cytoplasmic vesicle under high light-grown cells (Figures 6A–C and Supplementary Figure 4). It showed that the membrane structure is aberrant under high light, especially the *pgr11* and *pgr5* mutants. The majority of the thylakoid membranes were loosen in high light-grown cells. While in the WT cells, the thylakoid membranes are arranged as layers (stacked) in the chloroplast, with some membrane appressed. Recently we reported that photosynthetic efficiency is reduced under the high light condition in WT, *pgr11*, and *pgr5* mutants, which may be due to a change in chloroplast structure (Yadav et al., 2020). Such phenotype raised the question that mutant strains are defective in generating the functional membrane under high light conditions. The earlier report emphasized that autophagic bodies accumulate in plant cell vacuoles under Concanamycin A treatment since vacuolar hydrolase cannot act (Thompson et al., 2005). However, in our case, under high light conditions, we have observed a high degree of vacuolization and an increase of vacuole size in mutants (Figures 6A,B and Supplementary Figure 4). It was also being reported that vacuole lytic function is needed to synthesize TAG and lipid bodies in *C. reinhardtii* cells when subjected to light stress (Couso et al., 2018).

Carbohydrate Assay

Carbohydrate is a polysaccharide, and it is the storage form of sugars and starch in plants/algae. We quantified the carbohydrate content in WT, *pgr11*, and *pgr5* strains in normal and high light conditions. The carbohydrate content of WT and *pgr11*

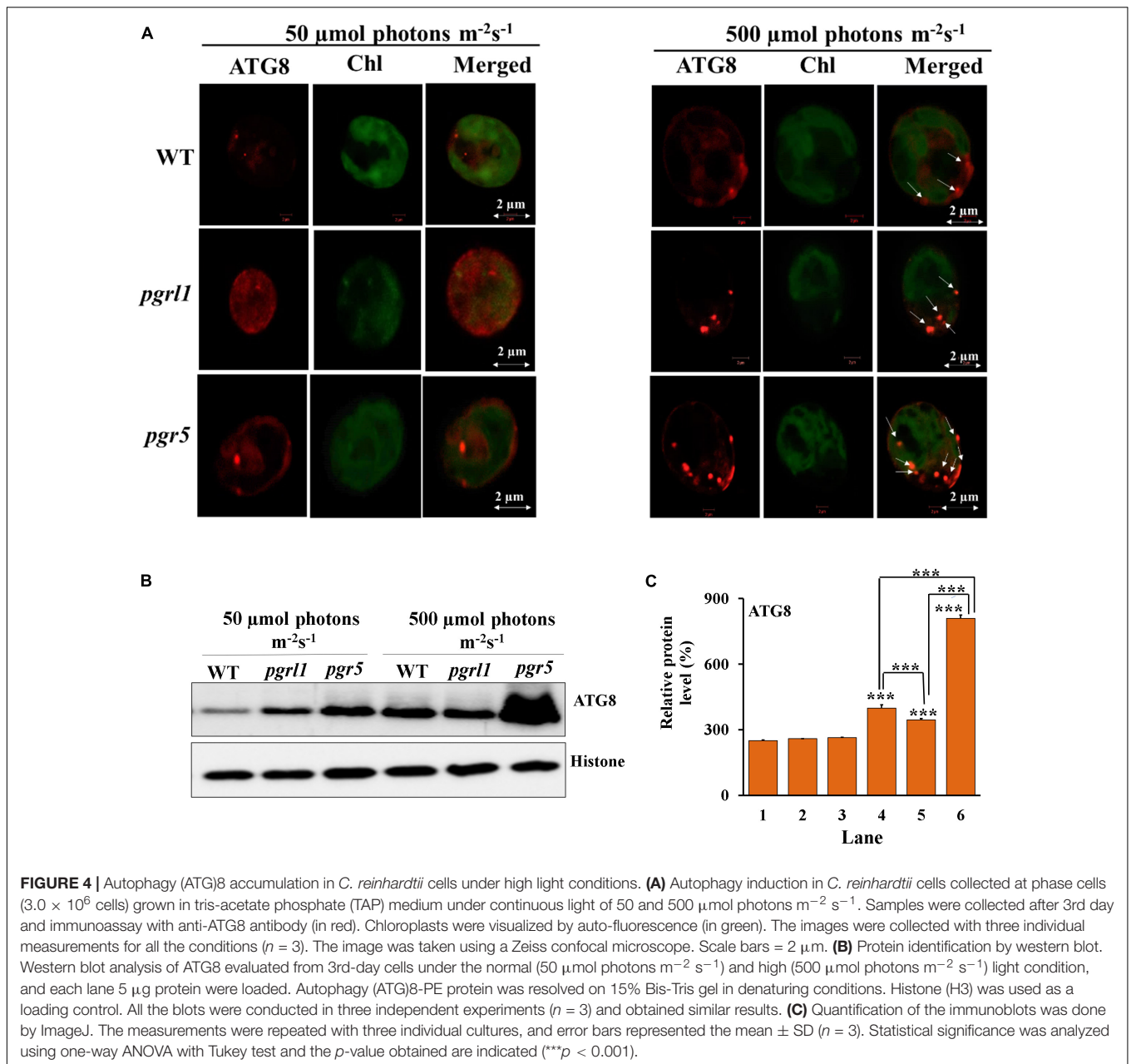


was increased significantly under the high light condition. The carbohydrate content was cross-checked with a starch deficient mutant (*sta6*) under normal light and high light. It shows about 8 μg of carbohydrate/10⁶ cells in standard and high light conditions (Figure 7) as measured with the anthrone reagent, which estimates starch and soluble sugars. Overall, our reports indicate that carbohydrate content has increased under the high light condition in WT and *pgr11*. However, it reduced in *pgr5* mutant under high light. Microalgae change their metabolism and convert excess energy into an energy-rich product such as lipid, starch, carbohydrate, or proteins under unfavorable conditions (Heredia-Arroyo et al., 2010). However, *pgr5* may have an altered NADPH and ATP ratio during photosynthesis, switching metabolic pathways that lead to lipid accumulation. These results indicate that high light induces the lipid pathways due to more energy equivalents in the *pgr5* mutant. Further,

we have tested the protein/enzyme of the lipid pathway from all the conditions.

Protein Analysis by Immunoblot

We have focused on the enzymes involved in the triacylglycerol (TAG) synthesis known as the Kennedy pathway. This pathway is mainly catalyzed by the acylation of diacylglycerols (DAGs) by diacylglycerol acyltransferases (DGAT), in which acyl-CoA is a substrate to form TAG. Acylation of diacylglycerols (DAGs) by phospholipid: diacylglycerol acyltransferase 1 (PDAT1) enzyme is the acyl-CoA independent pathway in the ER. To determine the involvement of PDAT and DGAT in high light response in *C. reinhardtii* and their protein level regulation was calculated (Figures 8A–C). The PDAT and DGAT were transiently upregulated in response to high light conditions. Protein expression was increased after the 3rd day, specifically

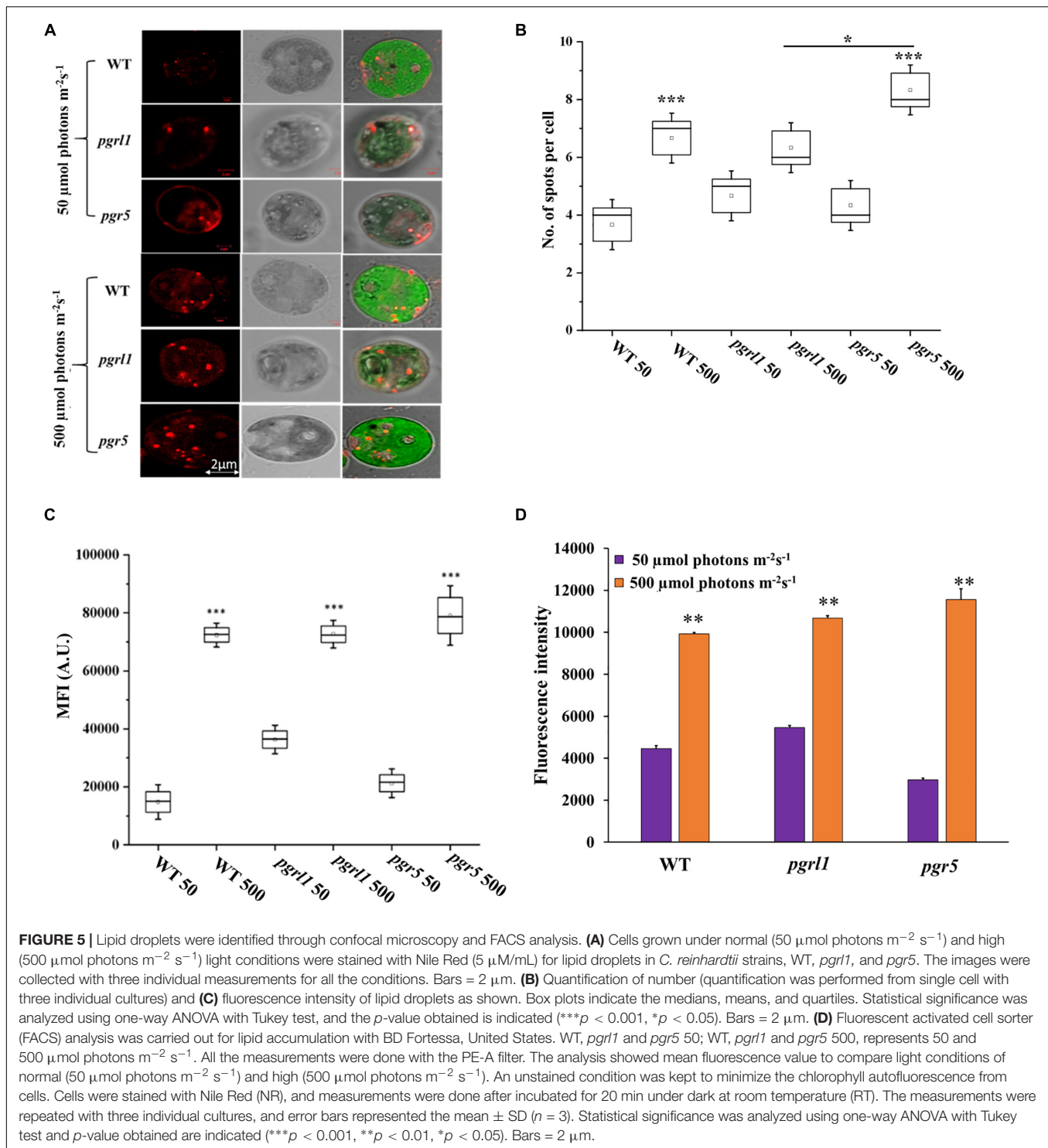


in *pgr5* expression of PDAT compared to *pgr11* (Figure 8A). Our results confirm an increase in TAG in *pgr11* and *pgr5* due to the enhanced content of PDAT and DGAT enzymes.

Fatty Acid Composition Under High Light Condition

Liquid chromatography/mass spectrometry (LC/MS) was used to analyze the fatty acids transesterification and the resultant fatty acid methyl esters (FAMES) from control strains WT, and mutants *pgr11* and *pgr5* under normal (50 $\mu\text{mol photons m}^{-2} \text{s}^{-1}$) and high light (500 $\mu\text{mol photons m}^{-2} \text{s}^{-1}$) cells (Table 1). Different compositions of fatty acids are observed in the high light grown *C. reinhardtii*. There was an increase in C16:1, C16:2,

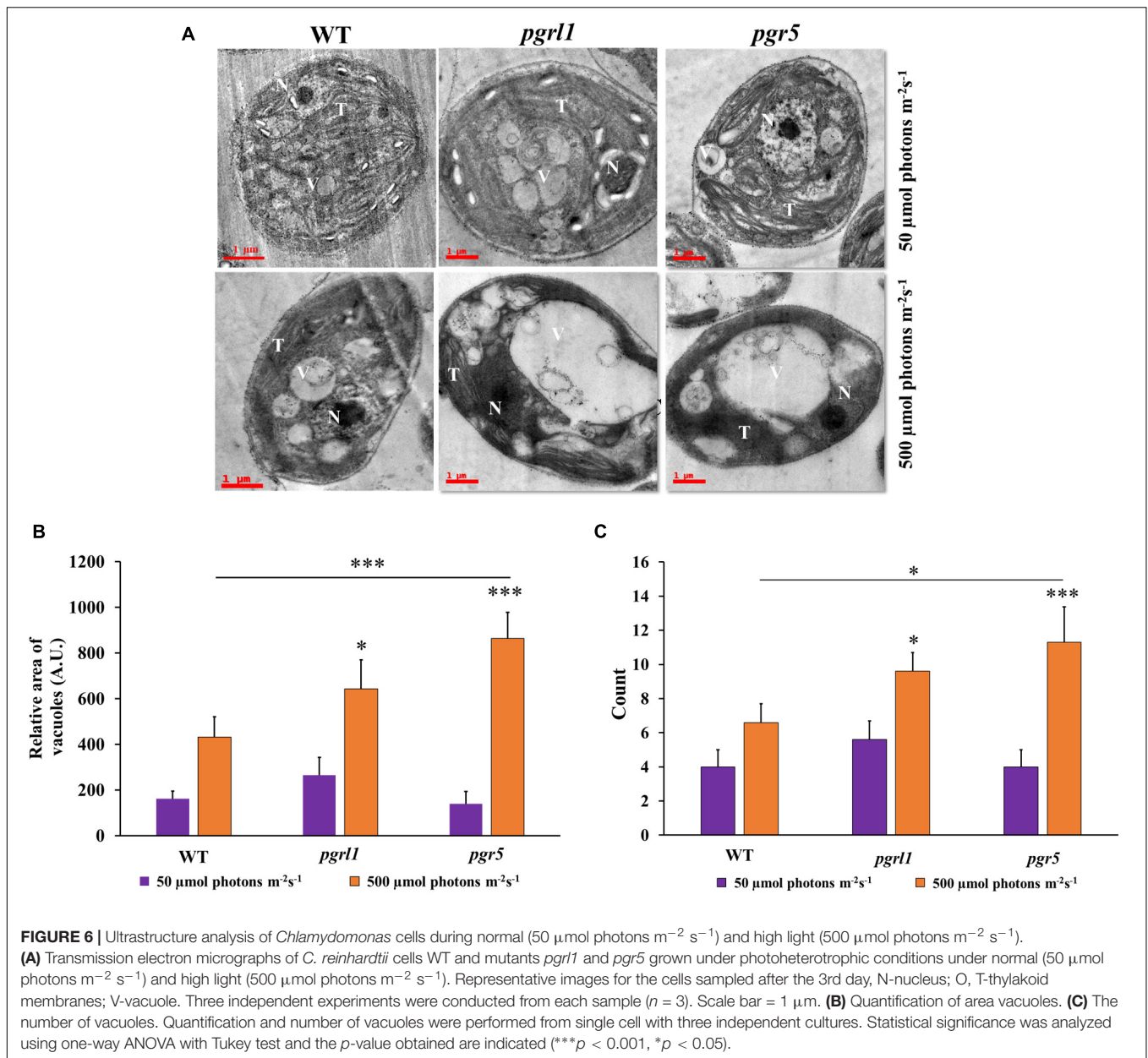
C16:3, C18:0, C18:1, and C18:3 in *pgr11* and *pgr5* mutant under high light conditions. We recently observed increasing total fatty acids in severe Fe deficiency from *C. reinhardtii* (Devadasu et al., 2019; Devadasu and Subramanyam, 2021). In our case also the total fatty acid content is significantly increased in *pgr11* and *pgr5* mutant strains. Overall saturated fatty acid increases from 6 to 10%, 13 to 18%, and 12 to 37% in WT, *pgr11*, and *pgr5* mutant, respectively, and monounsaturated fatty acid increases from 5 to 15%, 10 to 20%, and 12% to 38% in WT, *pgr11*, and *pgr5* mutant, respectively. However, there are also changes in total polyunsaturated fatty acids from 6 to 23%, 11 to 16%, and 17 to 27%. This result implies that high light increases SFA and MUFA in WT, *pgr11*, and *pgr5* mutant strains, but specifically, the SFA and MUFA increased significantly in *pgr5*.



Neutral Lipid and Membrane Lipid Analysis

To examine the fatty acid formed under high light, we studied the changes in neutral lipid, especially TAG and membrane lipid content and composition. We prepared neutral lipid extract from equal dry weights of WT, *pgr11*, and *pgr5* cells under 50

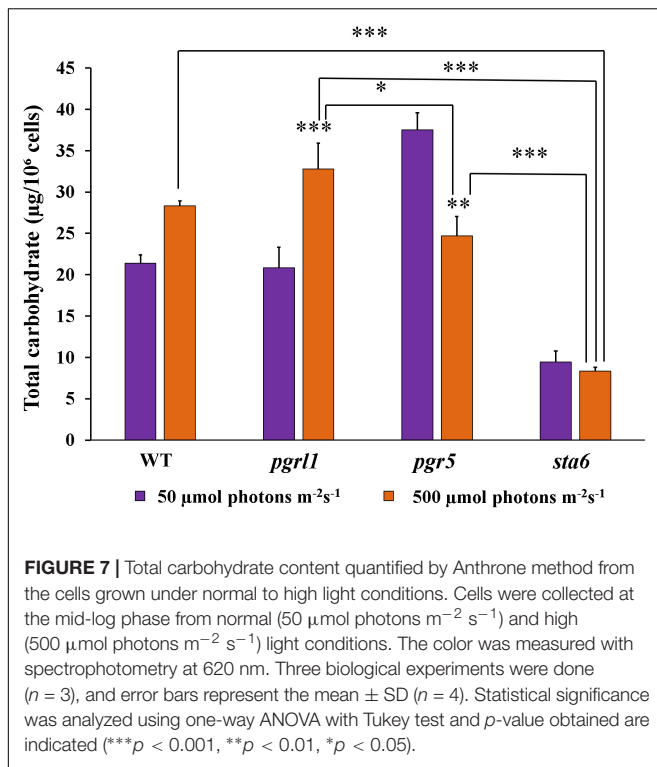
and $500 \mu\text{mol photon m}^{-2} \text{s}^{-1}$. Further, the extracted lipids were separated on TLC plates from the 3rd day of culture. This was stained with iodine, and results revealed that accumulation of more TAG was observed in *pgr5* compared to *pgr11* and WT (**Supplementary Figure 5**). To quantify the TAG, the TLC bands were recovered, and FAMES quantifies TAG content



through of GC (**Figure 9**). TAG concentration in WT and *pgr11* increased from 9 to 18%; however, *pgr5* significantly increased from 11 to 34% (**Figure 9D**). The fatty acid composition of TAG bands, 16:0, was raised in all strains under high light. However, the level of 18:0 was increased significantly in *pgr11* and *pgr5* mutants. Further, 18:1 ω 9c majorly increased in *pgr5* mutant under high light (**Figures 9A,D**). The accumulation of a significant amount of TAG in *pgr11* and *pgr5* under high light may suggest the role of membrane lipid in TAG synthesis (Fan et al., 2011).

To assess all the membrane lipids of *C. reinhardtii*, TLC is carried out. In WT, we observed not much change in chloroplast-specific lipid monogalactosyldiacylglycerol (MGDG), but chloroplast lipid digalactosyldiacylglycerol (DGDG) was

marginally increased. However, in *pgr5* mutant, MGDG and DGDG content reduced significantly under high light conditions (**Supplementary Figure 5**). Further GC quantification confirmed that the MGDG and DGDG were significantly decreased in high light (**Figures 9B,D**). The fatty acid composition shows that DGDG 18:1 and 18:1 ω 9c increased in *pgr11* mutant while decreased in *pgr5* mutant; however, not much change was observed in WT (**Figures 9C,D**). Further, the MGDG is enriched with C16:0, C18:1 ω 9c, C18:3, and C18:0. Not much change was seen in the fatty acid composition of MGDG in WT and *pgr11* but significantly decreased in *pgr5* under high light (**Figures 9B,D**). We assume that the reduced amounts of MGDG and DGDG are metabolized to TAG synthesis in *pgr5*, and a similar report was also observed from other studies



(Li et al., 2008; Devadasu and Subramanyam, 2021). The TLC and the GC data of membrane lipids support that the electron microscopic data that the stacks of thylakoids disturbed because of change in membrane lipids. Thus fatty acids from the chloroplasts and other intracellular membrane systems may have converted into TAG.

DISCUSSION

Cyclic electron transport around PSI requires the functions of PGRL1 and PGR5 to generate a proton gradient over the thylakoid membrane. PGR5 plays a regulatory role in cyclic electron flow around the PSI. It indirectly protects the PSI by enhancing photosynthetic control, a pH-dependent down-regulation of electron transfer at the Cyt *b6f* (Buchert et al., 2020). Less proton motive force across the thylakoid membrane and reduced cyclic electron transport around PSI suggest these protein's pivotal role in photosynthesis to protect it from high light (Yadav et al., 2020). Therefore, the CET is diminished in these mutants. It is known that CET plays a significant role in protecting plants in light stress. Recently, we reported that the photosynthetic activity was severely affected in *pgr11* and *pgr5* of *C. reinhardtii* when the cells were grown in high light (Yadav et al., 2020). We have also observed the non-photochemical quenching is substantially reduced in *pgr5*, which is supposed to protect the algae from high light that could harmlessly dissipate excess excitation energy as heat (Nama et al., 2019). When they grow in photoautotrophic conditions, the *pgr5* cells were much more sensitive to high light (500 $\mu\text{mol photon m}^{-2} \text{s}^{-1}$). To

our knowledge, in *pgr11* and *pgr5*, the autophagy-induced lipid accumulation has not been explored from high light conditions despite being well characterized on the photosynthesis. This study shows that autophagy induces lipid accumulation under high light in *pgr11* and *pgr5* mutants.

High Light Effect the Growth and Chlorophyll Content

Light is an essential factor in the production of biomass. Half of the microalgae species' dry weight is carbon and lipid (Zhu, 2015). This study demonstrates that high light intensity (500 $\mu\text{mol photons m}^{-2} \text{s}^{-1}$) enhanced the growth rate, promoted biomass and lipid accumulation of *C. reinhardtii* compared to regular light intensities in WT. However, growth and biomass were reduced in mutant (Figures 1B–D). PGRL1 and PGR5 proteins are essential in the acclimation process to high light. Thus, the growth curves show that the absence of these leads to less biomass and growth (Figure 1). In addition, the light stress response has been previously studied and shows the importance of light intensity in producing biomass and fatty acids in microalgae (Nzayisenga et al., 2020).

High Light Induces the Reactive Oxygen Species and Autophagy in *C. reinhardtii*

On the other hand, when microalgal cells were grown in high light, PSII undergoes severe damage. Hence photosynthetic electron transport chain induces the ROS (Li et al., 2009). Antioxidants usually accumulate in cells like carotenoids to repair the damage caused by ROS (Perez-Martin et al., 2014). Similarly, we also observed in our results that the total carotenoid content increased (Figure 2B). Interestingly, the ROS generation was much higher in *pgr5* because the lack of this gene led to acceptor side limitations as PGR5 is involved in protecting PSI. Thus, PSI's acceptor side is limited in *pgr5*. Because of acceptor side limitation, one could expect more ROS generation at the PSI acceptor side (Tiwari et al., 2016), suggesting that lipid synthesis could serve as a receptor to excess electrons to acclimatize to the abiotic stress. As already reported, oxidative stress causes lipid accumulation under nitrogen stress in microalgae (Yilancioglu et al., 2014).

Transmission electron microscopy (TEM) images of *C. reinhardtii* showed a pronounced increase in vacuoles' size under high light intensity, particularly in mutant strains (Figure 6). Accumulated autophagy bodies can play an essential role in lipid metabolism. A similar report was observed in nutrient limitations like nitrogen limiting conditions in *C. reinhardtii* (Couso et al., 2016). It has been reported that in stress conditions (like oxidative stress, rapamycin stress, and ER stress), the ATG8 gene was expressed in *C. reinhardtii* (Perez-Martin et al., 2014). In agreement with this hypothesis, we reported that significant expression of ATG8-PE protein was observed under high light conditions by immunofluorescence microscopy. It indicates that ATG8 is a pivotal protein to induce the autophagy process in *C. reinhardtii* (Figure 4). An abundance of ATG8-PE protein was increased in mutants due to high light, especially in *pgr5*. It seems an increase in stromal redox poise,

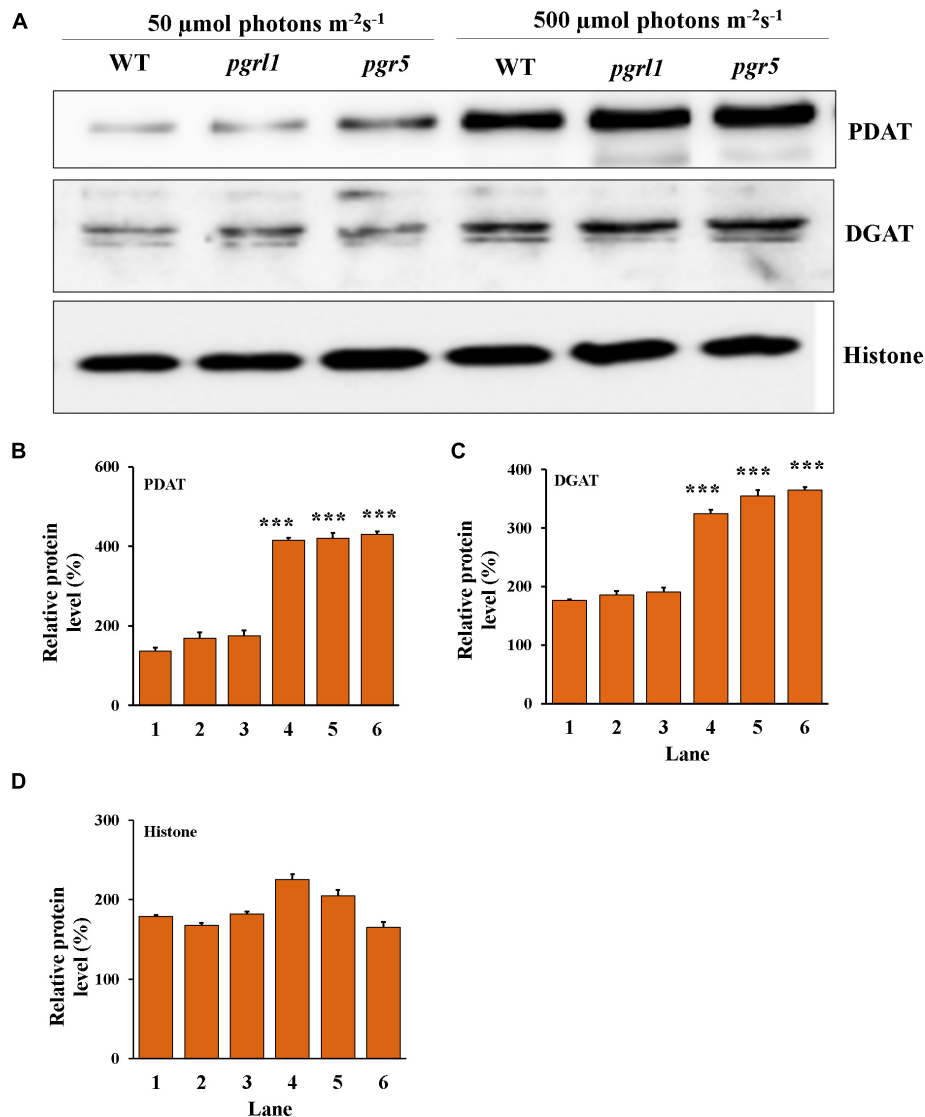
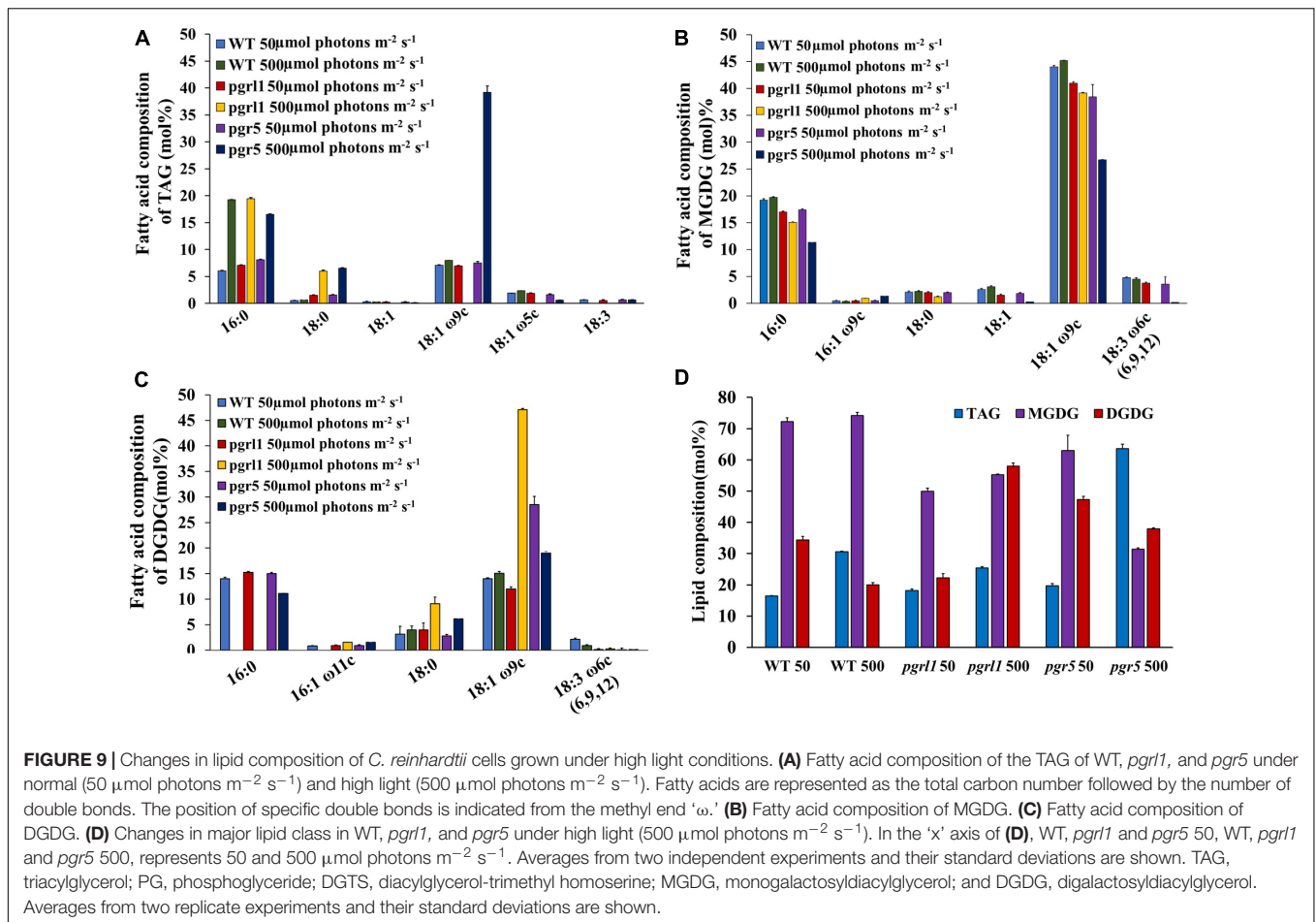


FIGURE 8 | Protein identification from western blot analysis. **(A)** The proteins were separated by denaturing gel electrophoresis, transferred to nitrocellulose membranes, and probed for the indicated proteins. Western blot analysis of Acyl-CoA: diacylglycerol acyltransferase (DGAT2A) and phospholipid diacylglycerol acyl-transferase (PDAT1) evaluated from 3rd-day cells under the normal ($50 \mu\text{mol photons m}^{-2} \text{s}^{-1}$) and high ($500 \mu\text{mol photons m}^{-2} \text{s}^{-1}$) light condition, and each lane ($5 \mu\text{g}$) protein were loaded on to 10% Bis-Tris gel in denaturing condition. Histone (H3) was used as a loading control. All the blots were in three independent times ($n = 3$) and obtained similar results. **(B)** Quantification of the immunoblots of PDAT, **(C)** DGAT and **(D)** histone. Data are expressed as mean \pm SD of 3 replicates. Statistical significance was analyzed using one-way ANOVA with Tukey test and p -value obtained are indicated ($***p < 0.001$).

which induces autophagy, thereby leading to triacylglycerol (TAG) accumulation. High light stress leads to ROS formation, which activates the autophagy mechanism. Increased ROS was seen in high light conditions; however, this was more prevalent in *pgr5* mutant when grown in high light, indicating that high light increases oxidative stress and autophagy, which accompanies increased lipid content in the cell.

The autophagy of *C. reinhardtii* contains numerous autophagy-related proteins. Among various ATG proteins, ATG8-PE protein is essential for forming autophagosomes (Pérez-Pérez et al., 2016). In this study, we measured the expression level of ATG8-PE protein to evaluate the autophagy

role in WT, *pgrl1*, and *pgr5* (Figure 4). ATG8 appeared as a faint band in the WT and mutants (*pgrl1* and *pgr5*) grown under optimal conditions ($50 \mu\text{mol photons m}^{-2} \text{s}^{-1}$), and it was increased when cells were exposed to high light. However, lipidated form ATG8-PE was detected in the *pgr5* mutant. Further, TEM confirmed several lytic vacuoles and small vesicles inside the vacuoles in high light treated cells (Figure 6). Under high light vacuoles size was markedly increased abundantly. This supports our hypothesis that light stress causes ROS production, especially in the *pgr5* mutant. In turn, ROS induces autophagy, as reported earlier, leading to an increase in lipid production. Confocal and fluorescent activated cell sorter (FACS) data also



suggested an increase in lipid droplet formation under high light in *pgr5* mutant (Figures 5A,D). Continuous light exposure leads to the accumulation of biomass and the cellular over reduction and formation of ROS, which induces autophagy and lipids in microalgae (Shi et al., 2017). Our previous results indicate that PSI and PSII were damaged when cells were grown in high light (Nama et al., 2019; Yadav et al., 2020). Based on this result, we interpret that lipid accumulation in mutant strains could be explained by PSII or PSI being over-reduced, leading to high ROS production. These increased ROS levels act as an autophagy inducer (Heredia-Martinez et al., 2018).

High Light Induces a High Amount of Lipids

In microalgae, lipid and carbohydrate are the primary energy storage forms and share the common carbon precursors for biosynthesis. Carbon partitioning is essential for the development of biofuels and chemicals. Most carbohydrates are stored as starch and sugars in microalgae. In several algal species, carbohydrate and lipid accumulate, while in some species, carbohydrate level decreases, and TAG increases, suggesting that lipids may be synthesized from carbohydrate degradation. Our results showed that both lipid and carbohydrate content increased in WT and *pgr11*. However, lipid accumulation precedes

carbohydrate accumulation (Figures 5, 7), consistent with the previous studies in the microalga, *Pseudochlorococcum*, under nitrogen stress conditions (Li et al., 2011). However, the carbohydrate content was reduced in *pgr5* mutant under high light growth, explaining that carbohydrate degradation would have been converted to lipids in *pgr5*. Therefore more lipid accumulation was observed. Complex metabolic regulations in the cell may control the accumulation of lipid droplets. The *pgr5* prevents the proton gradient and PSI dependant CET; therefore, the altered NADPH and ATP ratio may switch the metabolic pathways during the photosynthesis process. Some of the metabolic alterations would have converted to lipids, which is necessary to acclimatize to the high light in *pgr5*. Carbohydrate is the dominant sink for carbon storage in *C. reinhardtii* mutant, which lacks cell walls, so lipid synthesis occurs only when the carbon supply exceeds carbohydrate synthesis (Fan et al., 2012). Under saturating light, the *C. reinhardtii* culture induces lipid droplets formation without disrupting growth, while N starvation leads to significantly lower level (Goold et al., 2016).

In our case, a significant accumulation of TAG was observed in high light conditions and the accumulation of TAG is more in *pgr5* (Figure 5). In, *Arabidopsis thaliana* and *C. reinhardtii* TAG synthesis originated from multiple types of

acyltransferases. The final step of TAG biosynthesis was catalyzed by diacylglycerol acyltransferases (DGAT) and phospholipid diacylglycerol acyltransferase (PDAT) both involved in seed oil accumulation (Zhang et al., 2009). In the present study, we find the regulation of PDAT and DGAT at the protein level. Both the enzymes are accumulated under high light intensity, supporting these enzymes in the synthesis of TAG (Figure 8). Thus, the accumulation of TAG would be either through DGAT or PDAT routes.

High Light Alters the Fatty Acid Composition in *C. reinhardtii*

The fatty acid composition also plays a significant role in biofuel production. The results of total fatty acids show that the composition and content of fatty acids were different in WT, *pgr11*, and *pgr5* under normal and high light. The *pgr11* and *pgr5* have a higher percentage of SFA and MUFA under high light, as shown in Table 1. Palmitic (C16:0), stearic acid (C18:0), oleic acid content (C18:1), and palmitoleic (C16:1) increased in WT, *pgr11*, and *pgr5* under high light. This result implies high light stress conditions increase SFA and MUFA content in WT, *pgr11*, and *pgr5* mutant because the excess fatty acids could provide energy sink to the cells. Overall total fatty acid content was enhanced in *pgr5* mutant compared to WT and *pgr11*. We also observed an increase in the individual TAG band, especially the oleic acid (18:1 ω 9c) (Figure 9A). Usually, oleic acid is a source of carbon that requires a functional β -oxidation cycle in which oleic acid is reduced to acetyl-CoA then to sugars or synthesis of other fatty acids or lipids (Graham, 2008).

Interestingly, the thin layer chromatography results show that the membrane lipids have been decreased, which indicates that the degradation of these lipids could have converted to TAG, especially in *pgr11* and *pgr5* (Supplementary Figure 4). Also, the decreased fatty acids from MGDG and DGDG could have converted to TAG (Figure 9). Similar reports were observed suggesting the recycling of membrane lipids, monogalactosyldiacylglycerol (MGDG), and digalactosyldiacylglycerol (DGDG) into TAG accumulation in *C. reinhardtii* (Abida et al., 2015; Devadasu and Subramanyam, 2021). Therefore, we can interpret that fatty acids are dissociated from glycolipids, which are involved in the Kennedy pathway to synthesize the TAGs through the DGAT enzyme (Yoon et al., 2012).

Our results provided complete evidence that the two mutants, *pgr11* and *pgr5*, of *C. reinhardtii*, accumulate fatty acid and induced autophagy under high light conditions. The correlation between stress and TAG accumulation in photosynthesis of algae has been known for a century. Under high light conditions, these mutant's fatty acid compositions may be an important study for biotechnological applications. It suggests that one possible reason for the increase in lipid content may be the unbalanced redox state of the cells, leading to the generation of ROS. Therefore, the increased ROS levels in *pgr5* cells could play a dual role as signals to activate lipid biosynthesis and autophagy inducers to start recycling cellular components to fuel lipid production in this mutant (Tran et al., 2019). Therefore, *pgr11* and *pgr5* of

C. reinhardtii would be appropriate for producing high yield lipids (Lipids/TAG). Hence, our study could offer an essential value: microalgae-based lipid production can be promoted by applying various feedstocks to biodiesel and animal feed.

DATA AVAILABILITY STATEMENT

The original contributions presented in the study are included in the article/Supplementary Material, further inquiries can be directed to the corresponding author.

AUTHOR CONTRIBUTIONS

NC, ED, and RMY carried out the experiments, analyzed the data, and drafted the manuscript. RS designed the experiments, drafted the manuscript, and secured the fund. All authors approved the final version before submission.

FUNDING

RS was supported by the Institute of Eminence (UoH/IoE/RC1/RC1-20-019), Department of Biotechnology (BT/PR14964/BPA/118/137/2015), UGC-ISF Research Grant – File No. 6-8/2018 (IC), Council of Scientific and Industrial Research [No. 38 (1381)/14/EMR-II], and, DST-FIST and UGC-SAP, Government of India, for financial support.

ACKNOWLEDGMENTS

We thank Gilles Peltier, CEA – CNRS – Aix-Marseille Université, France, and Michael Hippler, University of Münster, Germany, for providing the mutants of *pgr11* and *pgr5*. We thank Dubuque Elizabeth Suzanne, Michigan State University, United States proofreading the manuscript.

SUPPLEMENTARY MATERIAL

The Supplementary Material for this article can be found online at: <https://www.frontiersin.org/articles/10.3389/fpls.2021.752634/full#supplementary-material>

Supplementary Figure 1 | Quantification of localization of ATG8 in *C. reinhardtii* cells under high light conditions from microscope image. Quantification of number of ATG8 from 50 μ mol photons $m^{-2} s^{-1}$ and 500 μ mol photons $m^{-2} s^{-1}$. Quantification was carried out from single cell with three individual cultures. Data are expressed as mean \pm SD of 3 replicates. Statistical significance was analyzed using one-way ANOVA with Tukey test and p -value obtained are indicated (** $p < 0.001$ and ** $p < 0.01$).

Supplementary Figure 2 | Lipid droplets were identified through confocal microscopy. Cells were grown under 50 μ mol photons $m^{-2} s^{-1}$ and 500 μ mol photons $m^{-2} s^{-1}$ were stained with Nile Red (5 μ M/mL) for lipid droplets in *C. reinhardtii* strains, WT, *pgr11*, and *pgr5*. The images were collected with three individual measurements for all the conditions. Scale bar = 20 μ m.

Supplementary Figure 3 | Neutral lipid content is quantified from the cells grown under normal and high light. Neutral lipid content was qualitatively measured with Nile Red fluorescence from the cells WT, *pgr1*, and *pgr5* grown with normal (50 $\mu\text{mol photons m}^{-2} \text{ s}^{-1}$) and high (500 $\mu\text{mol photons m}^{-2} \text{ s}^{-1}$) light condition stained with Nile Red on days 1–4. The measurements have been done with a microplate reader. Three biological experiments were done ($n = 3$). In 'x' axis WT, *pgr1* and *pgr5* 50; WT, *pgr1* and *pgr5* 500, represents 50 and 500 $\mu\text{mol photons m}^{-2} \text{ s}^{-1}$. Statistical significance was analyzed using one-way ANOVA, and subsequent Tukey's *post hoc t*-test and *p*-value obtained are indicated (** $p < 0.001$).

Supplementary Figure 4 | Ultrastructure analysis of *C. reinhardtii* cells during normal (50 $\mu\text{mol photons m}^{-2} \text{ s}^{-1}$) and high light (500 $\mu\text{mol photons m}^{-2} \text{ s}^{-1}$). Transmission electron micrographs of *C. reinhardtii* cells WT and mutants *pgr1* and *pgr5* grown under photoheterotrophic conditions under 50 $\mu\text{mol photons m}^{-2} \text{ s}^{-1}$ and 500 $\mu\text{mol photons m}^{-2} \text{ s}^{-1}$. Representative images were taken

after the 3rd day of growth. Three independent experiments were conducted from each sample ($n = 3$).

Supplementary Figure 5 | Alteration of membrane lipid and TAG in *C. reinhardtii* cells grown under normal and high light conditions. **(A)** TLC analysis showing TAG accumulation of *C. reinhardtii* cells WT and mutants *pgr1* and *pgr5* strains under 50 $\mu\text{mol photons m}^{-2} \text{ s}^{-1}$ and 500 $\mu\text{mol photons m}^{-2} \text{ s}^{-1}$. Three independent experiments were conducted for all samples ($n = 3$). **(B)** Separation of polar lipids by TLC from *C. reinhardtii* strains WT, *pgr1*, and *pgr5* under 50 $\mu\text{mol photons m}^{-2} \text{ s}^{-1}$ and 500 $\mu\text{mol photons m}^{-2} \text{ s}^{-1}$. Polar lipids and TAG was visualized by iodine staining. Three independent experiments were conducted for all samples ($n = 3$). WT, *pgr1* and *pgr5* 50, WT, *pgr1* and *pgr5* 500, represents 50 and 500 $\mu\text{mol photons m}^{-2} \text{ s}^{-1}$. TAG, triacylglycerol. DGDG, digalactosyldiacylglycerol; MGDG, monogalactosyldiacylglycerol; PC, phosphatidylcholine; PE, phosphatidylethanolamine; PG, phosphatidylglycerol; PI, phosphatidylinositol; SQDG, sulfoquinovosyldiacylglycerol.

REFERENCES

- Abida, H., Dolch, L.-J., Mei, C., Villanova, V., Conte, M., Block, M. A., et al. (2015). Membrane Glycerolipid Remodeling Triggered by Nitrogen and Phosphorus Starvation in *Phaeodactylum tricornutum*. *Plant Physiol.* 167, 118–136. doi: 10.1104/pp.114.252395
- Alishah Aratboni, H., Rafiei, N., Garcia-Granados, R., Alemzadeh, A., and Morones-Ramirez, J. R. (2019). Biomass and lipid induction strategies in microalgae for biofuel production and other applications. *Microb. Cell Fact.* 18:178. doi: 10.1186/s12934-019-1228-4
- Bligh, E. G., and Dyer, W. J. (1959). A rapid method for total lipid extraction and purification. *Can. J. Biochem. Physiol.* 37, 911–917.
- Bozzola, J. J., and Russell, L. D. (1998). *Electron Microscopy: principles and Techniques for Biologists*, 2nd Edn. Sudbury, MA: Jones and Bartlett publishers, 19–144.
- Buchert, F., Mosebach, L., Gäbelein, P., and Hippler, M. (2020). PGR5 is required for efficient Q cycle in the cytochrome *b6f* complex during cyclic electron flow. *Biochem. J.* 477, 1631–1650. doi: 10.1042/BCJ20190914
- Couso, I., Evans, B. S., Li, J., Liu, Y., Ma, F., Diamond, S., et al. (2016). Synergism between Inositol Polyphosphates and TOR Kinase Signaling in Nutrient Sensing, Growth Control and Lipid Metabolism in *Chlamydomonas*. *Plant Cell* 28, 2026–2042. doi: 10.1105/tpc.16.00351
- Couso, I., Pérez-Pérez, M. E., Martínez-Force, E., Kim, H.-S., He, Y., Umen, J. G., et al. (2018). Autophagic flux is required for the synthesis of triacylglycerols and ribosomal protein turnover in *Chlamydomonas*. *J. Exp. Bot.* 69, 1355–1367. doi: 10.1093/jxb/erx372
- Cuellar-Bermudez, S. P., Romero-Ogawa, M. A., Vannella, R., Lai, Y. S., Rittmann, B. E., and Parra-Saldivar, R. (2015). Effects of light intensity and carbon dioxide on lipids and fatty acid produced by *Synechocystis* sp. PCC6803 during continuous flow. *Algal Res.* 12, 10–16.
- Devadasu, E., Chinthapalli, D. K., Chouhan, N., Madireddi, S. K., Rasineni, G. K., Sripathi, P., et al. (2019). Changes in the photosynthetic apparatus and lipid droplet formation in *Chlamydomonas reinhardtii* under iron deficiency. *Photosynth. Res.* 139, 253–266. doi: 10.1007/s11120-018-0580-2
- Devadasu, E., Pandey, J., Dhokne, K., and Subramanyam, R. (2021). Restoration of Photosynthetic activity and supercomplexes from severe iron starvation in *Chlamydomonas reinhardtii*. *Biochim. Biophys. Acta Bioenerg.* 1862:148331. doi: 10.1016/j.bbapbio.2020.148331
- Devadasu, E., and Subramanyam, R. (2021). Enhanced lipid production in *Chlamydomonas reinhardtii* caused by severe Iron Deficiency. *Front. Sci.* 12:615577. doi: 10.3389/fpls.2021.615577
- Fan, J., Andre, C., and Xu, C. (2011). A chloroplast pathway for the de novo biosynthesis of triacylglycerol in *Chlamydomonas reinhardtii*. *FEBS Lett.* 585, 1985–1991. doi: 10.1016/j.febslet.2011.05.018
- Fan, J., Yan, C., Andre, C., Shanklin, J., Schwender, J., and Xu, C. (2012). Oil accumulation is controlled by carbon precursor supply for fatty acid synthesis in *Chlamydomonas reinhardtii*. *Plant Cell Physiol.* 53, 1380–1390. doi: 10.1093/pcp/pcs082
- Goold, H. D., Cuiné, S., and Légeret, B. (2016). Saturating Light Induces Sustained Accumulation of Oil in Plastidal Lipid Droplets in *Chlamydomonas reinhardtii*. *Plant Physiol.* 171, 2406–2417. doi: 10.1104/pp.16.00718
- Graham, I. A. (2008). Seed storage oil mobilization. *Annu. Rev. Plant Biol.* 59, 115–142. doi: 10.1146/annurev.arplant.59.032607.092938
- Heredia-Arroyo, T., Wei, W., and Hu, B. (2010). Oil accumulation via heterotrophic/mixotrophic *Chlorella protothecoides*. *Appl. Biochem. Biotechnol.* 162, 1978–1995. doi: 10.1007/s12010-010-8974-4
- Heredia-Martinez, L. G., Andres-Garrido, A., Martinez-Force, E., Perez-Perez, M. E., and Crespo, J. L. (2018). Chloroplast damage induced by the inhibition of fatty acid synthesis triggers autophagy in *Chlamydomonas*. *Plant Physiol.* 178, 1112–1129. doi: 10.1104/pp.18.00630
- Johnson, X., Steinbeck, J., Dent, R. M., Takahashi, H., Richaud, P., Ozawa, S.-I., et al. (2014). Proton gradient regulation 5-mediated cyclic electron flow under ATP- or redox- limited conditions: a study of Δ ATPase *pgr5* and Δ rbcl *pgr5* mutants in the green alga *Chlamydomonas reinhardtii*. *Plant Physiol.* 165, 438–452. doi: 10.1104/pp.113.233593
- Khotimchenko, S. V., and Yakovleva, I. M. (2005). Lipid composition of the red alga *Tichocarpus crinitus* exposed to different levels of photon irradiance. *Phytochemistry* 66, 73–79. doi: 10.1016/j.phytochem.2004.10.024
- Leister, D., and Shikanai, T. (2013). Complexities and protein complexes in the antimycin A- sensitive pathway of cyclic electron flow in plants. *Front. Plant Sci.* 4:161. doi: 10.3389/fpls.2013.00161
- Li, Y., Han, D., Sommerfeld, M., and Hu, Q. (2011). Photosynthetic carbon partitioning and lipid production in the oleaginous microalga *Pseudochlorococcum* sp. (*Chlorophyceae*) under nitrogen-limited conditions. *Bioresour. Technol.* 102, 123–129. doi: 10.1016/j.biortech.2010.06.036
- Li, Y., Horsman, M., Wang, B., Wu, N., and Lan, C. Q. (2008). Effects of nitrogen sources on cell growth and lipid accumulation of green alga *Neochloris oleoabundans*. *Appl. Microbiol. Biotechnol.* 81, 629–636. doi: 10.1007/s00253-008-1681-1
- Li, Z., Wakao, S., Fischer, B. B., and Niyogi, K. K. (2009). Sensing and responding to excess light. *Annu. Rev. Plant Biol.* 60, 239–260. doi: 10.1146/annurev.arplant.58.032806.103844
- Liu, Y., and Bassham, D. C. (2012). Autophagy: pathways for Self-Eating in Plant Cells. *Annu. Rev. Plant Biol.* 63, 215–223. doi: 10.1146/annurev-arplant-042811-105441
- Mandotra, S. K., Kumar, P., Suseela, M. R., Nayaka, S., and Ramteke, P. W. (2016). Evaluation of fatty acid profile and biodiesel properties of microalga *Scenedesmus abundans* under the influence of phosphorus, pH, and light intensities. *Bioresour. Technol.* 201, 222–229. doi: 10.1016/j.biortech.2015.11.042
- Mondal, M., Goswami, S., Ghosh, A., Oinam, G., Tiwari, O. N., Das, P., et al. (2017). Production of biodiesel from microalgae through biological carbon capture. *3 Biotech* 7:99. doi: 10.1007/s13205-017-0727-4
- Nama, S., Madireddi, S., Yadav, R., and Subramanyam, R. (2019). Non-photochemical quenching- dependent acclimation and thylakoid organization of *Chlamydomonas reinhardtii* to high light stress. *Photosynth. Res.* 139, 387–400. doi: 10.1007/s11120-018-0551-7

- Nzayisenga, J. C., Farge, X., Groll, S. L., and Sellstedt, A. (2020). Effects of light intensity on growth and lipid production in microalgae grown in wastewater. *Biotechnol. Biofuels* 13:4. doi: 10.1186/s13068-019-1646-x
- Pal, D., Khozin-Goldberg, I., Cohen, Z., and Boussiba, S. (2011). The effect of light, salinity, and nitrogen availability on lipid production by *Nannochloropsis* sp. *Appl. Microbiol. Biotechnol.* 90, 1429–1441. doi: 10.1007/s00253-011-3170-1
- Perez-Martin, M., Perez-Perez, M. E., Lemaire, S. D., and Crespo, J. L. (2014). Oxidative stress contributes to autophagy induction in response to endoplasmic reticulum stress in *Chlamydomonas*. *Plant Physiol.* 166, 997–1008. doi: 10.1104/pp.114.243659
- Pérez-Pérez, M. E., Florencio, F. J., and Crespo, J. L. (2010). Inhibition of Target of Rapamycin Signaling and Stress Activate Autophagy in *Chlamydomonas reinhardtii*. *Plant Physiol.* 152, 1874–1888. doi: 10.1104/pp.109.152520
- Pérez-Pérez, M. E., Lemaire, S. D., and Crespo, J. L. (2012). Reactive Oxygen Species and Autophagy in Plants and Algae. *Plant Physiol.* 160, 156–164. doi: 10.1104/pp.112.199992
- Pérez-Pérez, M. E., Lemaire, S. D., and Crespo, J. L. (2016). Control of Autophagy in *Chlamydomonas* is Mediated through Redox-Dependent Inactivation of the ATG4 Protease. *Plant Physiol.* 172, 2219–2234. doi: 10.1104/pp.16.01582
- Porra, R. J., Thompson, W. A., and Kriedemann, P. E. (1989). Determination of accurate extinction coefficients and simultaneous equations for assaying chlorophylls a and b extracted with four different solvents: verifying the concentration of chlorophyll standards by atomic absorption spectroscopy. *Biochim. Biophys. Acta* 975, 384–394. doi: 10.1016/s0005-2728(89)80347-0
- Ramundo, S., Casero, D., Mühlhaus, T., Hemme, D., Sommer, F., Crèvecoeur, M., et al. (2014). Conditional Depletion of the *Chlamydomonas* Chloroplast ClpP Protease Activates Nuclear Genes Involved in Autophagy and Plastid Protein Quality Control. *Plant Cell* 26, 2201–2222. doi: 10.1105/tpc.114.12.4842
- Shi, K., Gao, Z., Shi, T.-Q., Song, P., Ren, L.-J., Huang, H., et al. (2017). Reactive Oxygen Species-Mediated Cellular Stress Response and Lipid Accumulation in Oleaginous Microorganisms: the State of the Art and Future Perspectives. *Front. Microbiol.* 8:793. doi: 10.3389/fmicb.2017.00793
- Shikanai, T. (2014). Central role of cyclic electron transport around photosystem I in the regulation of photosynthesis. *Curr. Opin. Biotechnol.* 26, 25–30. doi: 10.1016/j.copbio.2013.08.012
- Shockey, J. M., Gidda, S. K., Chapital, D. C., Kuan, J.-C., Dhanoa, P. K., Bland, J. M., et al. (2006). Tung Tree DGAT1 and DGAT2 Have Nonredundant Functions in Triacylglycerol Biosynthesis and Are Localized to Different Subdomains of the Endoplasmic Reticulum. *Plant Cell* 18, 2294–2313. doi: 10.1105/tpc.106.043695
- Siaut, M., Cuiñé, S., Cagnon, C., Fessler, B., Nguyen, M., Carrier, P., et al. (2011). Oil accumulation in the model green alga *Chlamydomonas reinhardtii*: characterization, variability between common laboratory strains, and relationship with starch reserves. *BMC Biotechnol.* 11:7. doi: 10.1186/1472-6750-11-7
- Sorger, D., and Daum, G. (2002). Synthesis of triacylglycerols by the acyl-coenzyme A:diacyl-glycerol acyltransferase Dga1p in lipid particles of the yeast *Saccharomyces cerevisiae*. *J. Bacteriol.* 184, 519–524. doi: 10.1128/JB.184.2.519-524.2002
- Steinbeck, J., Nikolova, D., Weingarten, R., Johnson, X., Richaud, P., Peltier, G., et al. (2015). Deletion of Proton Gradient Regulation 5 (PGR5) and PGR5-Like 1 (PGRL1) proteins promote sustainable light-driven hydrogen production in *Chlamydomonas reinhardtii* due to increased PSII activity under sulfur deprivation. *Front. Plant Sci.* 6:892. doi: 10.3389/fpls.2015.00892
- Thompson, A. R., Doelling, J. H., Suttangkakul, A., and Vierstra, R. D. (2005). Autophagic Nutrient Recycling in Arabidopsis Directed by the ATG8 and ATG12 Conjugation Pathways. *Plant Physiol.* 138, 2097–2110. doi: 10.1104/pp.105.060673
- Tiwari, A., Mamedov, F., Grieco, M., Suorsa, M., Jajoo, A., Styring, S., et al. (2016). Photodamage of iron-sulphur clusters in photosystem I induces non-photochemical energy dissipation. *Nat. Plants* 2:16035. doi: 10.1038/nplants.2016.35
- Tolte, D., Ghysels, B., Alric, J., Petroustos, D., Tolstygina, I., Krawietz, D., et al. (2011). Control of hydrogen photoproduction by the proton gradient generated by cyclic electron flow in *Chlamydomonas reinhardtii*. *Plant Cell* 23, 2619–2630. doi: 10.1105/tpc.111.086876
- Towbin, H., Staehelin, T., and Gordon, J. (1979). Electrophoretic transfer of proteins from polyacrylamide gels to nitrocellulose sheets: procedure and some applications. *Proc. Natl. Acad. Sci. U. S. A.* 76, 4350–4354.
- Tran, Q. G., Cho, K., Park, S. B., Kim, U., Lee, Y. J., and Kim, H. S. (2019). Impairment of starch biosynthesis results in elevated oxidative stress and autophagy activity in *Chlamydomonas reinhardtii*. *Sci. Rep.* 9:9856. doi: 10.1038/s41598-019-46313-6
- Upadhyaya, S., Agrawal, S., Gorakshakar, A., and Rao, B. J. (2020). TOR kinase activity in *Chlamydomonas reinhardtii* is modulated by cellular metabolic states. *FEBS Lett.* 594, 3122–3141. doi: 10.1002/1873-3468.13888
- Van Doorn, W. G. (2011). Classes of programmed cell death in plants, compared to those in animals. *J. Exp. Bot.* 62, 4749–4761. doi: 10.1093/jxb/err196
- Wang, Z., and Benning, C. (2011). *Arabidopsis thaliana* Polar Glycerolipid Profiling by Thin Layer Chromatography (TLC) Coupled with Gas Liquid Chromatography (GLC). *J. Vis. Exp.* 49:2518. doi: 10.3791/2518
- Wase, N., Tu, B., Rasineni, G. K., Cerny, R., Grove, R., Adamec, J., et al. (2019). Remodeling of *Chlamydomonas* Metabolism Using Synthetic Inducers Results in Lipid Storage during Growth. *Plant Physiol.* 181, 1029–1049. doi: 10.1104/pp.19.00758
- Wellburn, A. R. (1952). The spectral determination of chlorophylls a and b, as well as total carotenoids, using various solvents with spectrophotometers of different resolution. *J. Plant Physiol.* 144, 307–313. doi: 10.1016/s0176-1617(11)81192-2
- Yadav, R., Aslam, S., Madireddi, S., Chouhan, N., and Subramanyam, R. (2020). Role of cyclic electron transport mutations pgr1 and pgr5 in acclimation process to high light in *Chlamydomonas reinhardtii*. *Photosynth. Res.* 146, 247–258. doi: 10.1007/s11120-020-00751-w
- Yeesang, C., and Cheirsilp, B. (2011). Effect of nitrogen, salt, and iron content in the growth medium and light intensity on lipid production by microalgae isolated from freshwater sources in Thailand. *Bioresour. Technol.* 102, 3034–3040. doi: 10.1016/j.biortech.2010.10.013
- Yilancioglu, K., Cokol, M., Pastirmaci, I., Erman, B., and Cetiner, S. (2014). Oxidative stress is a mediator for increased lipid accumulation in a newly isolated *Dunaliella salina* strain. *PLoS One* 9:91957. doi: 10.1371/journal.pone.0091957
- Yoon, K., Han, D., Li, Y., Sommerfeld, M., and Hu, Q. (2012). Phospholipid:diacylglycerol acyltransferase is a multifunctional enzyme involved in membrane lipid turnover and degradation while synthesizing triacylglycerol in the unicellular green microalga *Chlamydomonas reinhardtii*. *Plant Cell* 24, 3708–3724. doi: 10.1105/tpc.112.100701
- Zhang, M., Fan, J., Taylor, D. C., and Ohlrogge, J. B. (2009). DGAT1 and PDAT1 Acyltransferases have Overlapping Functions in Arabidopsis Triacylglycerol Biosynthesis and are Essential for Normal Pollen and Seed Development. *Plant Cell* 21, 3885–3901. doi: 10.1105/tpc.109.071795
- Zhekisheva, M., Boussiba, S., Khozin-Goldberg, I., Zarka, A., and Cohen, Z. (2002). Accumulation of Triacylglycerols in *Haematococcus pluvialis* is Correlated with that of Astaxanthin Esters. *J. Phycol.* 38, 40–41. doi: 10.1046/j.1529-8817.38.s1.9.x
- Zhu, L. (2015). Microalgal culture strategies for biofuel production: a review. *Biofuel Bioprod. Biorefin.* 9, 801–814. doi: 10.1002/bbb.1576

Conflict of Interest: The authors declare that the research was conducted in the absence of any commercial or financial relationships that could be construed as a potential conflict of interest.

Publisher's Note: All claims expressed in this article are solely those of the authors and do not necessarily represent those of their affiliated organizations, or those of the publisher, the editors and the reviewers. Any product that may be evaluated in this article, or claim that may be made by its manufacturer, is not guaranteed or endorsed by the publisher.

Copyright © 2022 Chouhan, Devadasu, Yadav and Subramanyam. This is an open-access article distributed under the terms of the Creative Commons Attribution License (CC BY). The use, distribution or reproduction in other forums is permitted, provided the original author(s) and the copyright owner(s) are credited and that the original publication in this journal is cited, in accordance with accepted academic practice. No use, distribution or reproduction is permitted which does not comply with these terms.